Modelling the Intake Manifold Dynamics in a Diesel Engine

Fredrik Karlsson

Modelling the Intake Manifold Dynamics in a Diesel Engine

Examensarbete utfört i Fordonssystem
vid Tekniska Högskolan i Linköping
av

Fredrik Karlsson

Reg nr: LiTH-ISY-EX-3084

Supervisor: **Thomas Stutte, DaimlerChrysler**

Examiner: **Prof. Lars Nielsen**

Linköping, April 2, 2001.

Avdelning, Institution Division, Department Vehicular Systems Dept. of Electrical Engineering		**Datum:** Date: April 2, 2001

Sammanfattning
Abstract

The goal is to model the intake manifold dynamics in a turbocharged diesel engine. Pressure and temperature are the central properties that are modeled and all models are physically based. The models are implemented and simulated in Simulink as part of a model representing a complete engine, namely the Mercedes-Benz OM611, a 2.2 liter four cylinder turbocharged diesel engine. A research car with this engine and an extensive measurement system is used to collect measurements needed for validation of the intake manifold models.

Three intake manifold models are presented and validated. All of them agree well with measurement data under the condition that exhaust gas recirculation is not active. When it is active however errors occurs, this is thought to be because of erroneous modelling of the EGR system.

Intake manifold models can be used for control and diagnosis purposes. This has become very important in recent years since tough legislations about lowering exhaust emissions, and detecting various faults has been made.

Abstract

The goal is to model the intake manifold dynamics in a turbocharged diesel engine. Pressure and temperature are the central properties that are modeled and all models are physically based. The models are implemented and simulated in Simulink as part of a model representing a complete engine, namely the Mercedes-Benz OM611, a 2.2 liter four cylinder turbocharged diesel engine. A research car with this engine and an extensive measurement system is used to collect measurements needed for validation of the intake manifold models.

Three intake manifold models are presented and validated. All of them agree well with measurement data under the condition that exhaust gas recirculation is not active. When it is active however errors occurs, this is thought to be because of erroneous modelling of the EGR system.

Intake manifold models can be used for control and diagnosis purposes. This has become very important in recent years since tough legislations about lowering exhaust emissions, and detecting various faults has been made.

Key word: Modelling, Intake manifold, MVEM, EGR.

Acknowledgments

Nomenclature

Symbol	Quantity	Unit
A_{Valve}	Effective area of EGR valve opening	m^2
c_p	Heat capacity at constant pressure	$J/(kg \cdot K)$
c_v	Heat capacity at constant volume	$J/(kg \cdot K)$
h	Enthalpy	J
h_{HT}	Heat transfer coefficient	W/K
m_{Air}	Mass of air in intake manifold	kg
m_{EGR}	Mass of exhaust gas in intake manifold	kg
$\dot{m}_{Air}$	Change of air mass in intake manifold	kg/s
$\dot{m}_{EGR}$	Change of exhaust gas mass in intake manifold	kg/s
$\dot{m}_{Inter}$	Change of air mass in intercooler	kg/s
$\dot{m}_{Intake}$	Change of total gas mass in intake manifold	kg/s
N_{Eng}	Engine speed	RPM
p_{Error}	Relative error in pressure simulation	$\%$
p_{Intake}	Intake manifold pressure	Pa
$\dot{p}_{Intake}$	Change of intake manifold pressure	Pa/s
$\dot{q}_{Intake}$	Rate of heat transfer in the intake manifold	J/s
R	Gas constant for intake manifold gas mix	$J/(kg \cdot K)$
R_{Air}	Gas constant for air	$J/(kg \cdot K)$
R_{Exh}	Gas constant for exhaust gas	$J/(kg \cdot K)$
T_{Amb}	Ambient temperature	K
T_{EGR}	Temperature of EGR flow after valve	K
T_{EGRC}	Temperature of EGR flow after cooler	K
T_{Error}	Relative error in temperature simulation	$\%$
T_{Exh}	Temperature of exhaust manifold	K
T_{Intake}	Intake manifold temperature	K
T_{Inter}	Temperature after intercooler	K
T_{Sim}	Simulation time	s
T_{Wall}	Intake manifold wall temperature	K
$\dot{T}_{Intake}$	Change of intake manifold temperature	K/s
u	Internal energy per mass unit	J/kg
U	Internal energy	J
V_{Eng}	Displaced volume	m^3
V_{Intake}	Intake manifold volume	m^3
W_{EGR}	Mass flow thru EGR pipe	kg/s
W_{Fuel}	Mass flow of fuel into cylinders	kg/s

Symbol	Quantity	Unit
W_{Inlet}	Mass flow into cylinders	kg/s
W_{Inter}	Mass flow after intercooler	kg/s
W_{Turb}	Mass flow thru turbine	kg/s
Z_{EGR}	EGR rate	%
$\gamma = c_p/c_v$	Ratio of heat capacities	-
ϵ_{EGRC}	EGR cooler efficiency	-
η_{Vol}	Volumetric Efficiency	-
ρ_{Intake}	Intake manifold density	kg/m^3

Abbreviations

CDI	Common rail Direct Injection
CI	Compression Ignited
ECU	Electronic Control Unit
EGR	Exhaust Gas Recirculation
F&E	Filling and Emptying
MVEM	Mean Value Engine Model
NOx	Nitrogen-oxide
OBD	On Board Diagnosis
RPM	Revolutions Per Minute (engine speed)
VGT	Variable Geometry Turbocharger

Contents

List of Figures

List of Tables

1 Introduction

The goal of this thesis is to model the intake manifold dynamics of a turbocharged diesel engine, and compare the simulated results with an existing model. Model accuracy and computational speed are both important. Without accuracy the model is less valuable, and if it requires a lot of computational power it will be too slow for practical use. The input signals to the model are taken from measurements done with the research car (see chapter 3).

The modelling and simulation are carried out in the Matlab/Simulink environment.

1.1 Background

In recent years a lot of work has been put into the field of Mean Value Engine Modelling (MVEM) and simulation of such models. The development is often driven by laws and legislations about lower fuel consumption and emissions. Also the increase in computational power during the last years has made modelling and simulation a powerful tool for developers in the automotive business. A model of the inlet manifold can be used in control applications, as well as for diagnosis purposes, such as an On Board Diagnosis (OBD) system. This system is for detecting faults, such as leaks in air paths, that increase the emissions and reduces the driveability of the car. An OBD system can consist of a model of the monitored part. This model is simulated on line and the simulation results are compared with measured values from the engine. This setup demands a correct model that do not require too much computational power, not always a simple equation.

1.2 Method

To capture the dynamic behavior of the pressure and temperature in the intake manifold a model containing different state equations is used. First a previously developed model is presented. This model uses pressure and mass in the manifold as states. In an attempt to improve the simulations a new model is derived from basically the same assumptions but with pressure and temperature in the manifold as states. The third model is an extension of the latter and includes heat transfer between the gases inside the manifold and the manifold walls. All three models are validated with measurement data from the research car.

1.3   Thesis outline

A short overview of the thesis and what the chapters contain are given in the following paragraphs.

Chapter 2, Turbocharged Diesel Engines A short introduction to diesel engines in general and the Mercedes-Benz OM611 engine in particular. Special features such as Exhaust Gas Recirculation (EGR) and Variable Geometry Turbocharger (VGT) are also explained here.

Chapter 3, The Research Car   An overview of the measurement system installed in the research car is given.

Chapter 4, Model Theory and Development   Different ways to model the intake manifold, and it's importance to the whole engine model is discussed. Three models of the intake manifold are derived.

Chapter 5, Generating Volumetric Efficiency Maps   The Volumetric Efficiency is discussed and two maps are created from different datasets.

Chapter 6, Model Validation   Validation of the intake manifold models using measurement data are performed. The different models are compared regarding both correctness of the simulated quantitys and computational speed.

Chapter 7, Extensions   Future work is discussed in this chapter.

Chapter 8, Conclusions   In this chapter the conclusions drawn from this work are presented and discussed.

2   Turbocharged Diesel Engines

The information about turbocharged diesel engines presented in this chapter, and much more, can be found in both [1] and [2]. Book [2] can indeed be recommended since it is specialized on turbocharged internal combustion engines. Useful information can also be found in [3], from where figure 2.1 originates.

Diesel engines, also known as Compression Ignition (CI) engines, have been turbocharged for more than five decades. It is the operating principle of the CI engine that enables them to be turbocharged without some of the problems occurring when turbocharging Spark Ignition (SI) engines. The basic idea of turbocharging is to increase the amount of air inducted in the cylinders. The more air you induct, the more fuel you can inject, and the more power output you get. A turbocharged engine can then be made smaller than a naturally aspirated engine which has the same power output, i.e. a turbocharged engine has a higher power to weight ratio. Other advantages is that pumping losses and friction decrease. There exists different ways to boost the intake air pressure. Either the air is compressed by a mechanically driven pump, or a turbine-compressor combination is used powered by energy from the exhaust gases. The Mercedes-Benz engine, used in this project, is equipped with the latter.

In a diesel engine the fuel is injected directly into the cylinder. Before the fuel is injected air is inducted and compressed in the cylinder. During compression the temperature is increased to over the self ignition temperature of the fuel. When combustion is required to start the fuel is injected, and after a small delay period when the liquid fuel evaporates and mixes with air, spontaneous ignition occurs. Since combustion starts before the whole amount of fuel is injected the possibility for negative effects such as knock is limited.

The operating principle of a four stroke CI-engine can be described in the following way. In figure 2.1 the movement of the piston and the valves are shown for the four strokes.

Intake stroke The intake valves are open and as the piston moves downwards the cylinder is filled with fresh air.

Compression stroke The intake valves closes and as the piston moves upwards the air in the cylinder is compressed. This causes the temperature to rise to about 800 K. In the end of this stroke the fuel is injected. The air temperature and pressure are above the fuels ignition point, therefore spontaneous ignition initiates the combustion process.

Expansion stroke Due to the high pressure created by the combustion

the piston is accelerated downwards. In the end the exhaust valves open.

Exhaust stroke The piston moves upwards and pushes the burned gases into the exhaust system. When the piston reaches its top position a new cycle starts.
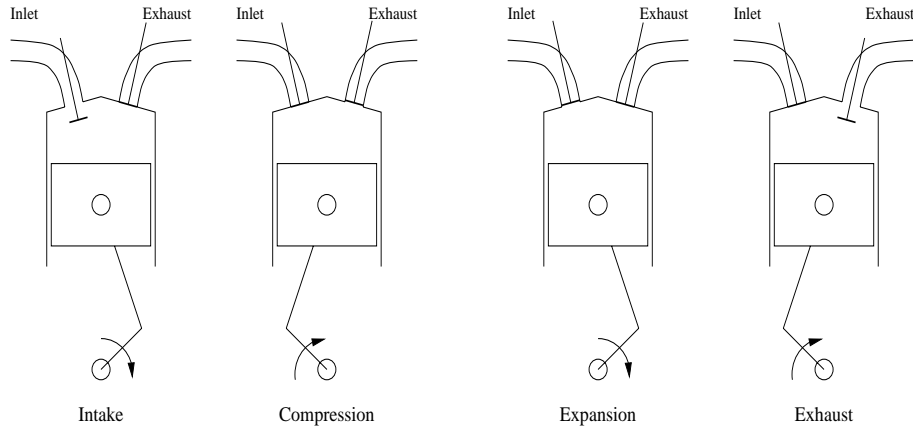
Figure 2.1: The four strokes of an internal combustion engine

2.1 The OM611 engine

The engine that is modelled in this master thesis is the Mercedes-Benz OM611. This is a 2.2 liter, 16 valve, four cylinder diesel engine with common rail direct injection (CDI) fitted in a Mercedes E-class. A schematic overview of the engine is given in figure 2.2. The engine has no throttle and is equipped with both Exhaust Gas Recirculation (EGR) and Variable Geometry Turbocharger (VGT). EGR and VGT will be described in the following sections.

2.2 Exhaust Gas Recirculation

The concept of EGR has been introduced as a way to decrease NO_x production. Since NO_x is mainly produced under high pressures and high temperatures, it is possible to control its formation by either reducing the compression or the temperature in the combustion chamber. When using EGR it is the temperature that is affected. EGR mixes cooled exhaust gas into the intake air stream, helping to lower combustion temperatures as less air and fuel are burned in each cycle.
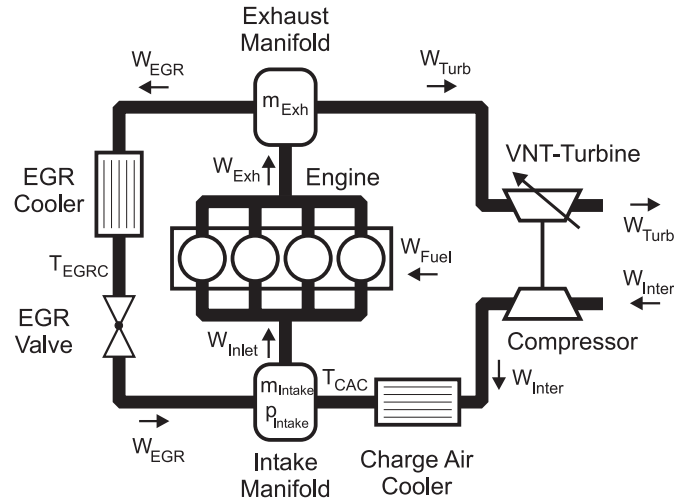
Figure 2.2: Schematic overview of the OM611 engine

One of the drawbacks with EGR is that it decreases the combustion stability. Because you don't want to loose driveability, i.e. power output, EGR is only active during low load conditions. The amount of EGR diesel engines can tolerate before misfire is up to 40 percent. The use of EGR reduces the formation of NO_x up to 30 percent.

2.3 Variable Geometry Turbocharger

A conventional turbocharger has a limited optimal working area. At low engine speeds there is not enough flow through the turbine to drive the turbocharger, and at high engine speeds some of the flow must bypass the turbine by a waste gate not to exceed the maximum rotational speed of the turbine. During accelerations from low engine speeds there is a time lag, called turbo lag, between the demand and the actual increase in acceleration. This lag exists because the turbine has to build up enough speed before the compressor can work effectively.

In order to widen the optimal working area, especially in the lower engine speeds, variable geometry turbocharging is applied. The basic idea is to have a variable inlet geometry to the turbine. This is managed by a set of vanes arranged in the path of the flow. By changing the angel of the vanes the inlet area to the turbine changes. During low engine speeds when the flow trough the engine is small one can increase the velocity of the flow

by partially closing the vanes, thus gaining turbine speed. With this setup there is also no more need for a waste gate.

In some literature the name variable nozzle turbocharger (VNT) is used.

2.4 Air Path System

In this section an overview of the air path system is given. The intake manifold is a small but important part of this system. Engine models are often based on the mass flow through the engine.

In figure 2.3 the air path system for the OM611 engine is presented. After entering the engine through the air filter (not shown in the figure), the air is compressed by the turbo charger (compressor). In the turbo charger the temperature of the air is also increased. This is an unwanted effect, so the air is then cooled in the charge air cooler (intercooler). Since there is no throttle the flow of air then directly enters the intake manifold where it can be mixed with recirculated exhaust gases. Then the air is inducted into the cylinders where combustion takes place. On the outlet side of the cylinders the exhaust gases enters the exhaust manifold, from where a portion of the gases can be recirculated through the EGR cooler back to the inlet manifold. The rest is led through the turbine (VGT) that drives the compressor and then through catalysts and silencer (not shown).
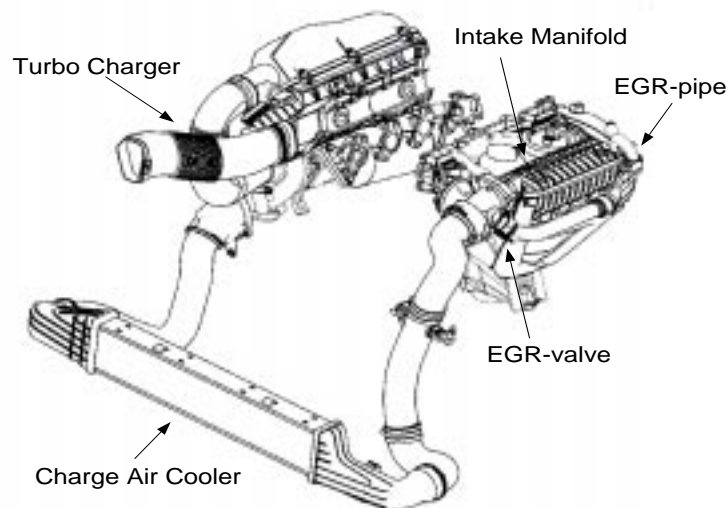
Figure 2.3: Overview of the air path system

3 The Research Car

The research car is a Mercedes E-class with the 2.2 liter diesel engine described in the previous section. A number of extra sensors has been installed in this engine to be able to closely monitor the behavior of certain parameters. The measurement system consists of five major components. An overview of them is given in figure 3.1.
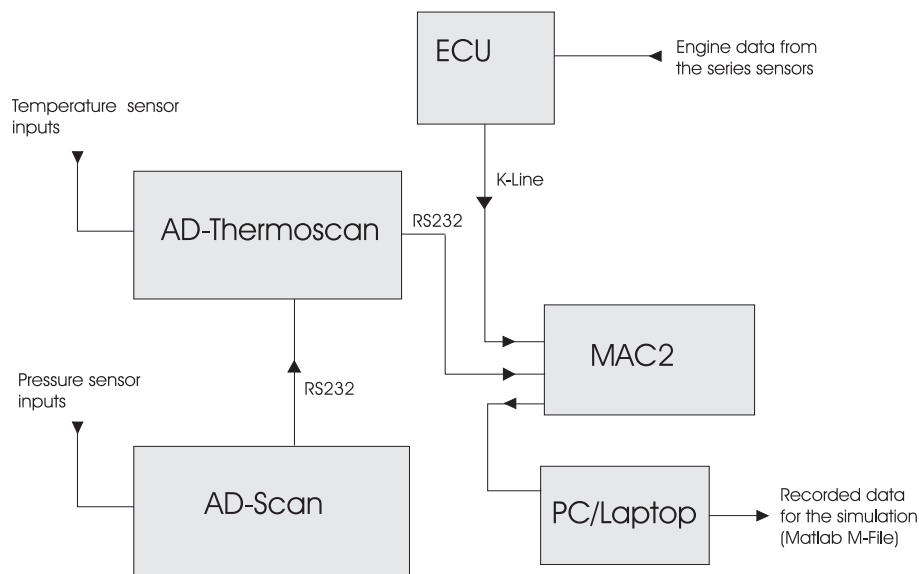
Figure 3.1: Schematic figure of the measurement components

3.1 The Mac2 measuring and application unit

For measuring and storing parameters from the research car a laptop computer is used. This computer has to be able to communicate with the Engine Control Unit (ECU) and the additional measuring equipment installed. To do this the Mac2 unit is used as an interface. Measuring data is gathered by the ECU and the additional sensors and sent via the Mac2 unit to the laptop. In the laptop it is stored and can be saved as a Matlab m-file. The software used for this application is called INCA and it is distributed by ETAS GmbH [4]. This software is also used for controlling the engine via

the ECU and to change the programming of the ECU.

3.2 The engine control unit (ECU)

The standard ECU usually integrated with this engine has been exchanged for a modified ECU. This ECU is equipped with an extra Flash-EPROM memory. This is done to allow modifications in the engine control program. Modifications to the control program was done a couple of times during the work on this thesis. For example the EGR valve had to be set in a closed position during some measurements, and the ability to specify the amount of fuel to be injected was used while doing measurements on a roll testbed.

3.3 The AD-Thermoscan

The AD-Thermoscan is used for temperature measurements. It has fourteen channels that can be connected to thermal elements, in this case K-elements ($N_iC_r - Ni$). The resolution of the temperature measurement can be chosen between two ranges depending on whether a high resolution is wanted over a shorter range or a lower resolution over a longer range. The two ranges are from -25°C to 1250°C with a resolution of 5°C, or from -50°C to 205°C with a resolution of 1°C. Which range is used depends on where the sensor is located, both ranges are used in this measurement system. The device is produced by CSM GmbH.

3.4 The AD-Scan

The AD-Scan is similar to the AD-Thermoscan, but it is used for pressure measurement. The pressure sensors connected to the measuring channels are so called expansion stripe elements. They transform a change of pressure to a change in resistance. The change of resistance causes a voltage change which is what the AD-Scan handles. With this setup pressures ranging from 500 mBar to 4000 mBar can be measured.

4 Model Theory and Development

The simulation model used in this thesis is based on the OM611 engine described is section 2.1. This is a model simulating the complete engine and it was developed by Ricardo Consulting Eng. Ltd [5] and DaimlerChrysler [6]. In this model the engine is represented by a lumped parameter model based on quasi steady-state flow assumptions. The non-steady flow energy equation is applied in which heat transfer to the environment and changes in flow kinetic energy are neglected. This method of modeling combine physical principles with the use of steady state maps [7].

As can be seen in figure 4.1 the model is divided in different subsystems. The work in this thesis is concentrated on the intake manifold, which is a subsystem of the inlet system. The rest of the engine model will, with a few exceptions, be viewed only as a simulation package.

The engine model has been optimized at DaimlerChrysler for the purpose of diagnosis [8]. It is this model that is the basis in this thesis.
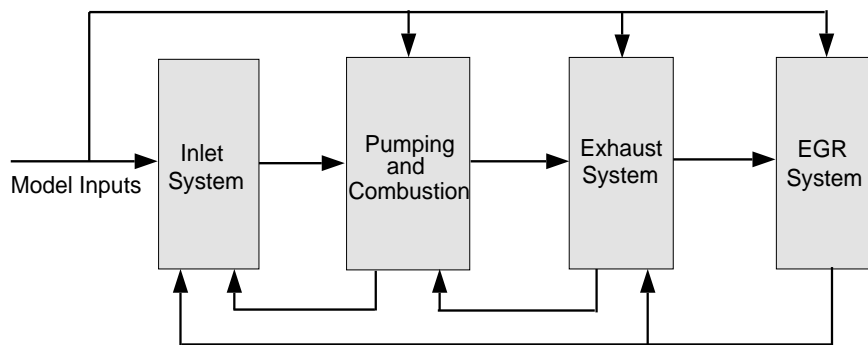
Figure 4.1: Overview of subsystems in simulink model

4.1 Intake Manifold Model

Modelling the intake manifold in a correct way is important because this system governs the flow into the engine's cylinders. This flow is crucial to engine performance since the amount of air inducted into the cylinders to a large extent governs the amount of fuel that can be burned, and therefore the power output. The amount of air in the intake manifold depends mainly on three factors: the flow into the manifold (from intercooler and EGR valve), the flow into the cylinders, and the inlet manifold pressure. The flow into

the cylinders is determined by a parameter called volumetric efficiency, see chapter 5.

The intake manifold can be viewed as a reservoir. Flows from both the intercooler (W_{Inter}) and the EGR valve (W_{EGR}) are entering the reservoir and the flow into the cylinders (W_{Inlet}) is leaving the reservoir, see figure 4.2.
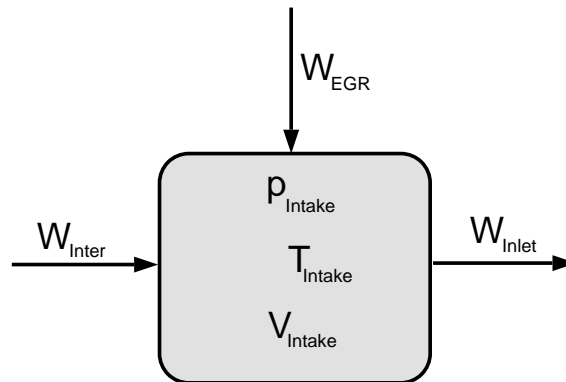
Figure 4.2: Intake manifold

Three intake manifold models will be derived and discussed in the following sections. The first model uses pressure and mass in the manifold as states and the other two uses pressure and temperature. EGR is included in all models and in the last one heat transfer is also included. These models are so called Mean Value Engine Models (MVEMs). They are dynamic, physically based and simplified models. They describe the time development of desired variables on a time scale a little larger than an engine cycle, so cycle to cycle variations of the parameters are not captured. MVEMs are often used when designing model based engine control systems and for diagnosis.

To generate the models Filling and Emptying (F&E) modelling is used. With this method the gas state in the manifold, or any control volume, is defined by mass and energy conservation equations along with information on the mass flow rates into and out of the manifold. This method assumes a number of simplifications. The pressure, temperature and composition inside the manifold are assumed homogeneous. Also instant and perfect mixing of incoming flow with matter inside the manifold is assumed.

By using conservation of mass in the manifold and the ideal gas law a very simple intake manifold model can be obtained. This model consists of

one manifold pressure state equation and the assumption that the intake
manifold temperature is constant ([9], [10]). In an engine equipped with a
turbocharger and EGR however the assumption of constant temperature is
not correct. This leads to also considering the conservation of energy in the
manifold.

As input signals to the intake manifold models the following parameters
are needed: $W_{Inter}, T_{Inter}, W_{EGR}, T_{EGR}$ and N_{Eng}. For the model including
heat transfer the intake manifold wall temperature, T_{Wall}, is also needed.
However, a measurement of this temperature was not available so an approx-
imation was used instead (see section 6.2.3). All input signals are measured
with the research car except for W_{EGR} which is taken from the EGR model
(see section 4.5).

4.2   p & m State Model

In this section the pressure and mass state model is presented. This model
uses pressure and mass in the intake manifold as states. An adiabatic as-
sumption is made, i.e. heat transfer in the mainfold is neglected.

A short derivation of the state equations are made here, a more thorough
one can be found in [11].

We will have two gases mixing inside the volume, the fresh air from the
intercooler and the recirculated exhaust gas . But when we derive the state
equations we will treat the two gas components separately, see figure 4.3.

When we treat the two gas components separately we assume that each
of them has, in the intake manifold, the partial pressure p_i, the mass m_i
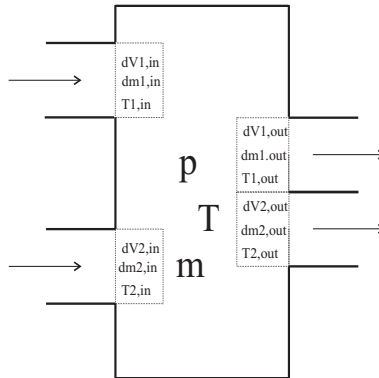
Figure 4.3: Intake manifold with two gas components.

and the gas constant R_i. The temperature T and volume V are the same for both gas components. Applying the ideal gas law gives us

$$p_i V = m_i R_i T \tag{4.1}$$

We will now consider one of the gas components, called component 1. Assume that during the short time interval dt, a small volume $dV_{1,in}$ is pushed into the reservoir. The work to push this volume into the reservoir can be assumed to be

$$p dV_{1,in} = dm_{1,in} R_1 T_{1,in} \tag{4.2}$$

The gas also carries the internal energy (per mass unit)

$$u_{1,in} = c_{v1} T_{1,in} \tag{4.3}$$

There is also a flow out of the reservoir of gas component 1. For this flow it holds that

$$\begin{aligned} p dV_{1,out} &= dm_{1,out} R_1 T_{1,out} = dm_{1,out} R_1 T \\ u_{1,out} &= c_{v1} T_{1,out} = c_{v1} T \end{aligned} \tag{4.4}$$

By using equations 4.2-4.4 and the relation $c_p = c_v + R$ we can write the non-steady energy equation for gas component 1

$$\begin{aligned} dU_1 &= dm_{1,in} c_{v1} T_{1,in} + dm_{1,in} R_1 T_{1,in} - dm_{1,out} c_{v1} T_{1,out} - dm_{1,out} R_1 T_{1,out} \\ &= dm_{1,in} c_{p1} T_{1,in} - dm_{1,out} c_{p1} T_{1,out} \end{aligned} \tag{4.5}$$

It also holds that

$$\begin{aligned} dp_1 V &= dm_1 R_1 T + m_1 R_1 dT = R_1 (dm_1 T + m_1 dT) \\ dU_1 &= dm_1 c_{v1} T + m_1 c_{v1} dT = c_{v1} (dm_1 T + m_1 dT) \end{aligned} \tag{4.6}$$

For gas component 1 it then holds that

$$\frac{c_{v1} dp_1 V}{R_1} = dm_{1,in} c_{p1} T_{1,in} - dm_{1,out} c_{p1} T \tag{4.7}$$

By letting W_1 denote the mass flow, we can rewrite this relation as

$$\dot{p}_1 = \frac{R_1 c_{p1}}{V c_{v1}} \left(W_{1,in} T_{1,in} - W_{1,out} T \right) \tag{4.8}$$

This is the pressure state equation when we have only one gas component. For the current system with two gas components we have

$$\dot{p} = \dot{p}_1 + \dot{p}_2 = \frac{R_1 c_{p1}}{V c_{v1}} \left(W_{1,in} T_{1,in} - W_{1,out} T \right) + \frac{R_2 c_{p2}}{V c_{v2}} \left(W_{2,in} T_{2,in} - W_{2,out} T \right)$$
(4.9)

By letting subscript 1 denote the air, and subscript 2 denote the recirculated exhaust gas in the manifold and the assumption that

$$\begin{aligned} W_{1,out} &= \frac{m_1}{m_1+m_2} W_{out,tot} \\ W_{2,out} &= \frac{m_2}{m_1+m_2} W_{out,tot} \end{aligned}$$
(4.10)

we can rewrite the pressure state equation in the following way

$$\dot{p}_{Intake} = \frac{1}{V_{Intake}} \Big(\frac{R_{Air} c_{pAir}}{c_{pAir} - R_{Air}} W_{Inter} T_{Inter} + \frac{R_{Exh} c_{pExh}}{c_{pExh} - R_{Exh}} W_{EGR} T_{EGR}$$
$$- \left((1 - Z_{EGR}) \frac{R_{Air} c_{pAir}}{c_{pAir} - R_{Air}} + Z_{EGR} \frac{R_{Exh} c_{pExh}}{c_{pExh} - R_{Exh}} \right) W_{Inlet} T_{Intake} \Big)$$
(4.11)

where

$$Z_{EGR} = \frac{m_{EGR}}{m_{Air} + m_{EGR}}$$
(4.12)

When we have two inflowing gases we get two mass balance equations

$$\begin{aligned} \dot{m}_{Air} &= W_{Inter} - (1 - Z_{EGR}) W_{Inlet} \\ \dot{m}_{EGR} &= W_{EGR} - Z_{EGR} W_{Inlet} \end{aligned}$$
(4.13)

Since we now have the pressure and mass in the manifold we can use the ideal gas law to calculate the temperature

$$\begin{aligned} T_{Inter} &= \frac{p_{Intake} V_{Intake}}{(m_{Air} + m_{EGR}) \frac{m_{Air} R_{Air} + m_{EGR} R_{EGR}}{m_{Air} + m_{EGR}}} \\ &= \frac{p_{Intake} V_{Intake}}{m_{Air} R_{Air} + m_{EGR} R_{EGR}} \end{aligned}$$
(4.14)

Equations (4.11) and (4.13) together form the pressure and mass state equations model including EGR.

The implementation of this model into simulink can be seen in appendix B in figures B.1 and B.2.

4.3   p & T State Model

In this model we will use pressure and temperature in the intake manifold as states. Heat transfer in the manifold is neglected, i.e. we have an adiabatic assumption. We also assume perfect mixing of the air and EGR flow in the manifold and that air and exhaust gas properties are equal. The latter assumption results in the following simplifications

$$c_v = c_{vAir} = c_{vExh}$$
$$c_p = c_{pAir} = c_{pExh}$$
$$R = R_{Air} = R_{Exh}$$

When EGR is included conservation of mass in the manifold requires that

$$\dot{m}_{Intake} = W_{Inter} + W_{EGR} - W_{Inlet} \tag{4.15}$$

Applying conservation of energy to equation (4.15) leads to the equation

$$W_{Inter} \cdot h_{Air} + W_{EGR} \cdot h_{EGR} - W_{Inlet} \cdot h_{Inlet}$$
$$= \tfrac{d(m \cdot u)}{dt} = W_{Inlet} c_v T_{Intake} + m_{Intake} c_v \dot{T}_{Intake} \tag{4.16}$$

Equation (4.16) can now be rewritten in the following way by using that the enthalpy can be expressed as $h_x = T_x R \gamma / (\gamma - 1)$

$$\dot{T}_{Intake} = \frac{W_{Inter} T_{Inter} R \gamma}{(\gamma - 1) m_{Intake} c_v} + \frac{W_{EGR} T_{EGR} R \gamma}{(\gamma - 1) m_{Intake} c_v}$$
$$- \frac{W_{Inlet} T_{Intake} R \gamma}{(\gamma - 1) m_{Intake} c_v} - \frac{W_{Inlet} T_{Intake}}{m_{Intake}} \tag{4.17}$$

By using the ideal gas law $pV = mRT$ and the fact that $c_v = R/(\gamma - 1)$ this equation can be written as

$$\dot{T}_{Intake} = \frac{W_{Inter} T_{Inter} R \gamma T_{Intake}}{p_{Intake} V_{Intake}} + \frac{W_{EGR} T_{EGR} R \gamma T_{Intake}}{p_{Intake} V_{Intake}}$$
$$- \frac{W_{Inlet} T_{Intake}^2 R \gamma}{p_{Intake} V_{Intake}} - \frac{W_{Inlet} T_{Intake}^2 R}{p_{Intake} V_{Intake}} \tag{4.18}$$

The final form of the temperature differential equation can now be written by applying mass conservation from equation (4.15). This leads to the equation

$$\dot{T}_{Intake} = \frac{RT_{Intake}^2}{p_{Intake}V_{Intake}}\Big[W_{Inter}\left(\gamma\frac{T_{Inter}}{T_{Intake}} - 1\right)$$
$$+W_{EGR}\left(\gamma\frac{T_{EGR}}{T_{Inter}} - 1\right) - W_{Inlet}\left(\gamma - 1\right)\Big] \qquad (4.19)$$

The inlet manifold pressure state equation can now be deduced. To do this we use the differentiation of the ideal gas law applied to the mass of gas in the intake manifold

$$\dot{p}_{Intake} = \frac{R}{V_{Intake}}\left(\dot{m}_{Intake}T_{Intake} + m_{Intake}\dot{T}_{Intake}\right) \qquad (4.20)$$

and equation (4.19). This results in the following equation

$$\dot{p}_{Intake} = \frac{\gamma RT_{Intake}}{V_{Intake}}\left(W_{Inter}\frac{T_{Inter}}{T_{Intake}} + W_{EGR}\frac{T_{EGR}}{T_{Intake}} - W_{Inlet}\right) \qquad (4.21)$$

Equations (4.19) and (4.21) together form the temperature and pressure state equation model including EGR.

How this model is implemented in simulink is shown in appendix B figures B.3 and B.4. For simulating this model the heat transfer coefficient (h_{HT}) is set to zero.

4.4   Heat Transfer Model

In the models deduced in the previous sections we have made an adiabatic assumption, i.e. no heat transfer occurs between the gases in the intake manifold and the intake manifold walls. For a naturally aspirated engine without a EGR system this assumption might very well be valid. In this case when there is a turbocharger and EGR present however, the temperatures in the manifold will vary over a wider range and reach higher values, and heat transfer may be important to include.

The model presented there is a natural extension of the model deduced in the previous section. The same assumptions are made except that heat transfer is taken into account when the equations are derived.

Conservation of mass in the manifold requires

$$\dot{m}_{Intake} = W_{Inter} + W_{EGR} - W_{Inlet} \qquad (4.22)$$

Using the differentiation of the ideal gas law we get the relation

$$\dot{p}_{Intake} = \frac{R}{V_{Intake}} \left(W_{Inter} + W_{EGR} - W_{Inlet} \right) + \frac{p_{Intake}}{T_{Intake}} \dot{T}_{Intake} \qquad (4.23)$$

Applying energy conservation to the intake manifold gives

$$\frac{d(mc_vT)_{Intake}}{dt} = W_{Inter}c_pT_{Inter} + W_{EGR}c_pT_{EGR} - W_{Inlet}c_pT_{Intake} - \dot{q}_{Intake}$$
$$(4.24)$$

The effect of heat transfer is here captured by the term $\dot{q}_{Intake}$. It consists of the heat transfer coefficient (h_{HT}) and the temperature difference between the gas inside the manifold and the manifold walls ($T_{Intake} - T_{Wall}$), see equation 4.27.

Rearranging equation 4.24 results in the temperature state equation

$$\dot{T}_{Intake} = \frac{RT_{Intake}^2}{p_{Intake}V_{Intake}} \Big[(\gamma \frac{T_{Inter}}{T_{Intake}} - 1)W_{Inter} + (\gamma \frac{T_{EGR}}{T_{Intake}} - 1)W_{EGR}$$
$$-(\gamma - 1)W_{Intake} - \frac{\dot{q}_{Intake}}{c_vT_{Intake}} \Big] \qquad (4.25)$$

Inserting equation (4.25) in (4.23) results in the pressure state equation

$$\dot{p}_{Intake} = \frac{\gamma RT_{Intake}}{V_{Intake}} \Big[\frac{T_{Inter}}{T_{Intake}} W_{Inter}$$
$$+ \frac{T_{EGR}}{T_{Intake}} W_{EGR} - W_{Inlet} - \frac{\dot{q}_{Intake}}{c_pT_{Intake}} \Big] \qquad (4.26)$$

Equations (4.25) and (4.26) together form the pressure and temperature state equations for the model including heat transfer and EGR. The expression for $\dot{q}_{Intake}$ is

$$\dot{q}_{Intake} = h_{HT} \left(T_{Intake} - T_{Wall} \right) \qquad (4.27)$$

where h_{HT} is the heat transfer coefficient and T_{Wall} is the intake manifold wall temperature.

The implementation of equations 4.25 and 4.26 into simulink can be seen in appendix B figures B.3 and B.4.

4.5 EGR Model

The EGR system consists of a connection between the exhaust manifold and the intake manifold. Thru this connection exhaust gases are recirculated to the intake system. To make the EGR more effective an intercooler is used to cool the exhaust gas before it mixes with the fresh intake air. The cooled exhaust gas is injected into the air flow thru a valve just before the intake manifold. An overview of the EGR system is given in figure 4.4.
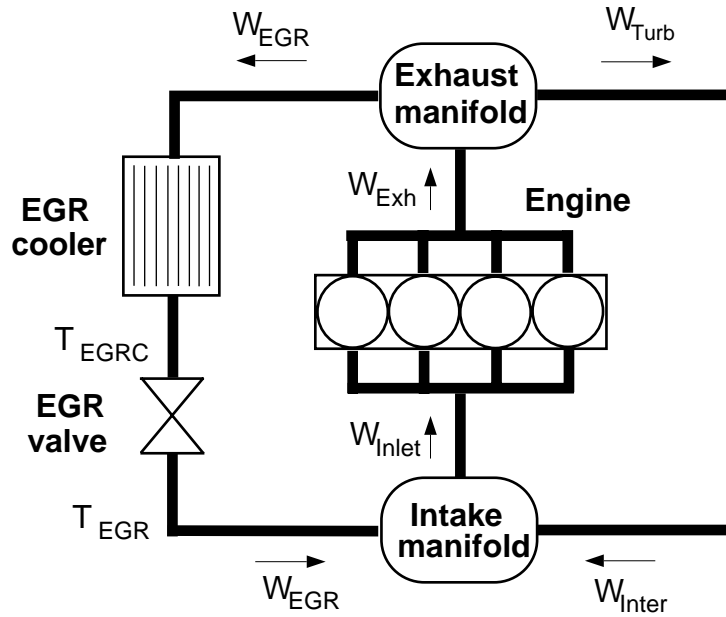

Figure 4.4: Schematic overview of the EGR system

The system is modelled in two parts, the EGR cooler and the EGR valve flow. In the cooler model only the temperature change is regarded, the pressure in the cooler is assumed to be equal to the pressure in the exhaust manifold. The cooler is modelled as a simple heat exchanger and the exit temperature of the EGR cooler can be predicted by

$$T_{EGRC} = T_{Exh} - \epsilon_{EGRC}(T_{Exh} - T_{Cool}) \tag{4.28}$$

where ϵ_{EGRC} is the EGR cooler efficiency. The EGR cooler efficiency is implemented as a two dimensional look up table and is a function of engine speed and the mass flow through the EGR system.

$$\epsilon_{EGRC} = f(N_{Eng}, W_{EGR}) \tag{4.29}$$

However, it was found out that the model for the EGR cooler worked very poorly and it was replaced by a sensor that measures the temperature directly after the intercooler. This means that the temperature T_{EGRC} is a direct input to the model.

In the valve flow model two basic equations are used for the flow and temperature of the gas flowing thru the valve:

$$W_{EGR} = A_{Valve} \frac{p_{Exh}}{\sqrt{T_{Exh}}} \psi \left(\frac{p_{Intake}}{p_{Exh}} \right)$$
$$T_{EGR} = \left(\frac{p_{Intake}}{p_{Exh}} \right)^{\frac{\gamma-1}{\gamma}} T_{EGRC} \tag{4.30}$$

The effective area of the valve opening (A_{Valve}) is an important parameter. It is modeled as a lookup table where the control signal from the ECU is the input signal. The data for the lookup table was provided by the valve-supplier. It has to be investigated further whether this lookup table is correct.

Except for the usual form of EGR called external EGR there is also internal EGR. This is the backflow of exhaust gases from the cylinders into the intake manifold. It is assumed that these gases will be concentrated around the intake ports so the influence on the manifold is neglected.

5 Generating Volumetric Efficiency Maps

There exists no easy way to measure the mass flow at the intake ports without changing the characteristics of the manifold. So instead models of varying complexity is used to calculate the port mass flow from other variables. The model used in this thesis is the so called speed-density equation, a simple and common model. This equation states that the mass of air flowing into the cylinders equals the volume flow of the engine, times the air density. But since the engine is not a perfect pump, a correction term is needed. This dimensionless constant is called the volumetric efficiency and it measures the effectiveness of an engines ability to induce air from the intake manifold into the cylinders. It is defined as the ratio of the actual volume flow rate of air entering the cylinders and the rate at which volume is displaced by the piston. So the expression for the volumetric efficiency becomes:

$$\eta_{Vol} = 120 \frac{W_{Inlet}}{N_{Eng} \rho_{Intake} V_{Eng}} \tag{5.1}$$

In the model the volumetric efficiency is implemented as a 2D lookup table. The flow into the cylinders can be rewritten in terms of inlet manifold density by using the expression for η_{vol} and the lookup table:

$$W_{Inlet} = \frac{\eta_{Vol} N_{Eng} \rho_{Intake} V_{Eng}}{120} \tag{5.2}$$

To create a volumetric efficiency map the following parameters are needed: W_{Inter}, T_{Intake}, p_{Intake} and N_{Eng}. If the EGR is active during the measurement you also need the EGR rate Z_{EGR}.

The volumetric efficiency maps presented in this chapter are created in the following way. Measurement data from all the variables and operating points are implemented as vectors in a matlab m-file. Break points for engine speed and intake manifold density is chosen. This set of break points create a grid covering the operating range of the engine. The intake manifold density is calculated for each operating point using $\rho_{Intake} = p_{Intake}/(R_{Air} \cdot T_{Intake})$. If EGR is active the EGR flow is calculated using $W_{EGR} = W_{Inter} \cdot Z_{EGR}/(100 - Z_{EGR})$. For each operating point the corresponding value of the volumetric efficiency is calculated using equation (5.1). Because of static conditions while measuring the data W_{Inlet} consists of $W_{Inter} + W_{EGR}$. The volumetric efficiency can now be seen as a function of engine speed and inlet manifold density and therefore presented as a 3D surface, see figures 5.1 and

5.2 for examples. Interpolation is used to find values in between measured points.

This way of implementing the volumetric efficiency is straight forward and computationally fast, but it requires a thorough mapping of the engine under static conditions. Another way to predict the intake port mass flow, without the need for static engine mapping, is presented in [12]. In this paper the quantity air charge per stroke is modeled instead of the volumetric efficiency.

5.1   Using engine testbed data

Measurement data from an OM611 engine in a testbed was used to create this map. The data was taken from a database. The measurements are performed by running the engine at a fix engine speed with a fix fueling value. For each combination of engine speed and fueling the needed parameters are measured after the values has stabilized. The EGR system was active during this measurement. The EGR-rate was measured using a CO_2 analysis.

The engine speed break points is set in the range of 1000-4500 rpm, in steps of 500 rpm. At each of these engine speeds we have eight different fueling conditions ranging from low to near maximum fueling. This gives us a set of 64 operating points that encloses most of the engines operating range. η_{Vol} is now represented by the map shown in figure 5.1.

This volumetric efficiency map was found out to work quite poorly with the model, as we will see in the validation chapter. To improve the results an empirically based correction was implemented in the simulink model. The corrections in the map significantly improved the model output.

5.2   Using roll testbed data

Since the volumetric efficiency map generated from the engine testbed data was not correct for the engine in the research car, we decided to generate a new map. The basis for this map is measurements with the research car on a roll testbed. Eight engine speeds were selected and for each engine speed seven different fueling conditions was set. To achieve static running conditions the amount of fuel injected was controlled by a laptop via the ECU. Unfortunately the brake in the roll testbed was not strong enough to let us gather all the measurements needed on low engine speeds. That is why this map is only valid down to engine speeds around 2000 rpm. The map is extended by extrapolation to engine speeds down to 1500 rpm. This was
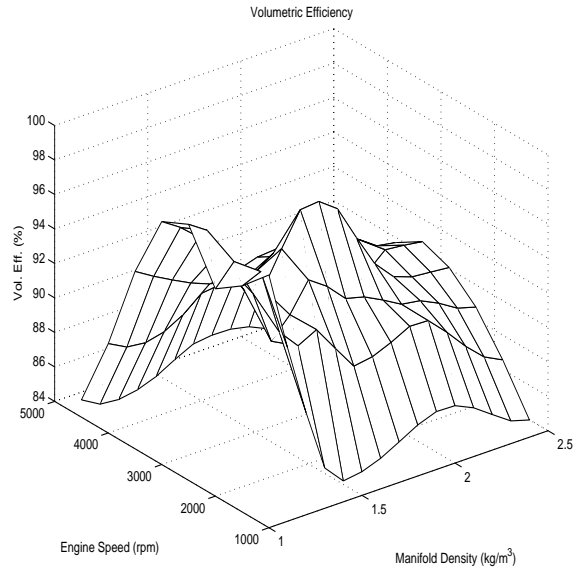
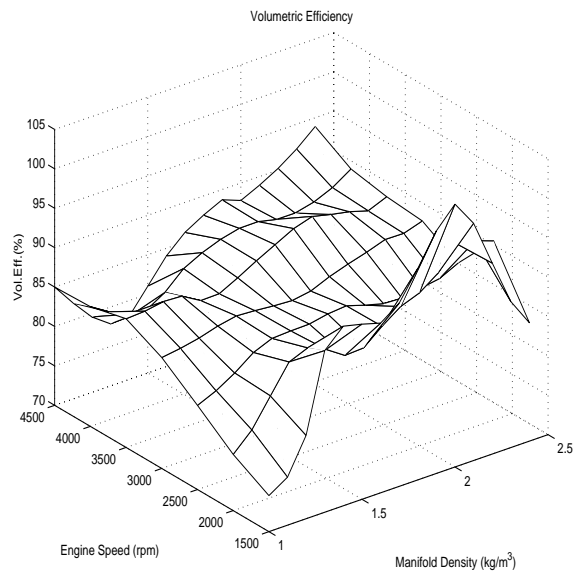Figure 5.1: Volumetric Efficiency map generated from testbed data

Figure 5.2: Volumetric Efficiency map generated from roll testbed data

made to allow simulation of more test data and one must keep in mind that
the map may not be totally correct in this region. However, simulations
have shown good results. The EGR system was turned off during this
measurement. The reason for this is that in contrast to an engine testbed
it was not possible to measure the EGR-rate directly in the car. However,
the influence of the EGR is included in the map since the map is a function
of the intake manifold density which is mostly effected by the EGR. The
generated map is shown in figure 5.2.

6 Model Validation

The different models of the intake manifold presented in this thesis are validated in this chapter. The validation is made by comparing the simulated quantity's with measurements made in the engine. The generated volumetric efficiency maps will also be validated using one of the intake manifold models.

6.1 Validation of volumetric efficiency maps

Since there is no way to measure the actual flow of air into the cylinders the validation can not be done by comparing the simulated air flow with a measured one. Validation is instead performed in the following way:
The p & m state model is simulated with a number of different measurement files using all three volumetric efficiency maps (see chapter 5), all other parameters are kept constant. The pressure in the intake manifold is then compared for the different simulations. The differences in the simulations are then only due to the differences in the volumetric efficiency maps.

This method for validation only tells us which map that fits our model best and nothing about the maps ability to predict the air flow into the cylinders in a correct way. By assuming that the rest of the model is correct however, this tells us that the map should also be correct. Another way to validate the volumetric efficiency map would be to use a more complex model of the intake manifold. Such a model could be based on the Navier and Stoke equations, which can describe a number of the complex phenomena occurring inside the manifold [13].

The volumetric efficiency map is generated from steady-state data, but it is also used to predict port air mass flow during transient operation. So the assumption that a transient trajectory consists of a series of steady-state operating points is made. Since this is just an approximation an error might be involved. This error, along with others such as inertial effects, wave effects, heat transfer, backflow and friction are discussed in [13] and found to be quite small.

Only one of the measurement files used for validation is presented here. In figure 6.1 the engine speed profile of this file is shown. As can be seen this measurement consists of both dynamic and near constant parts. The EGR system in not active.
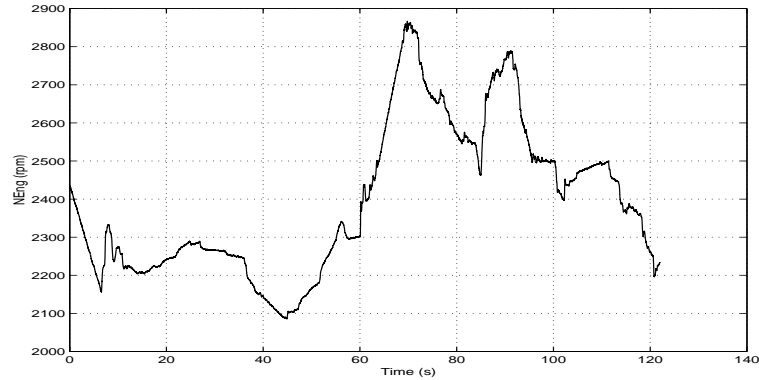
Figure 6.1: Engine speed profile of validation file

6.1.1   Map from engine testbed

First the map based on the engine testbed data is validated. Figure 6.2 shows the measured and simulated intake manifold pressure. The profile of the simulated pressure seems to fit the measurement quite well, but it is much to low. This might be because the prediction of the port air mass flow is to high, thus making the simulated pressure in the intake manifold drop. It can also be seen that the error is smaller when the pressure is higher, which is shown in figure 6.3 where the relative error is presented. It is obvious that the error in the pressure simulation when this map is used is too large for any practical use.
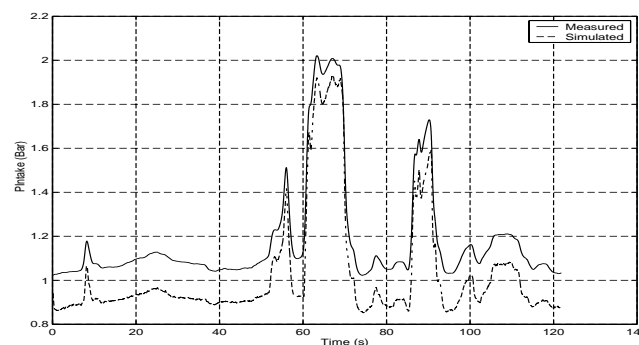
Figure 6.2: Pressure simulation using map based on engine testbed data
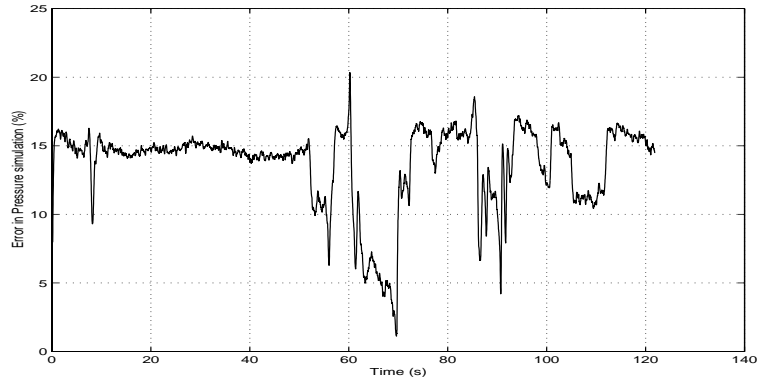
Figure 6.3: Relative error in pressure simulation using map based on engine testbed data

6.1.2 Modified map from engine testbed

The pressure simulation and the corresponding relative error with the modified map are shown in figure 6.4 and 6.5 respectively. A major improvement from the previous simulation can be seen. The simulated pressure is always a bit to high but it follows the measured pressure signal very accurately. Again the error is smaller when we have high pressures.
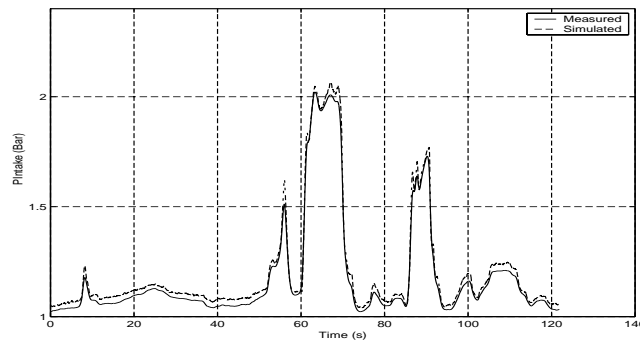
Figure 6.4: Pressure simulation using the modified engine testbed data map
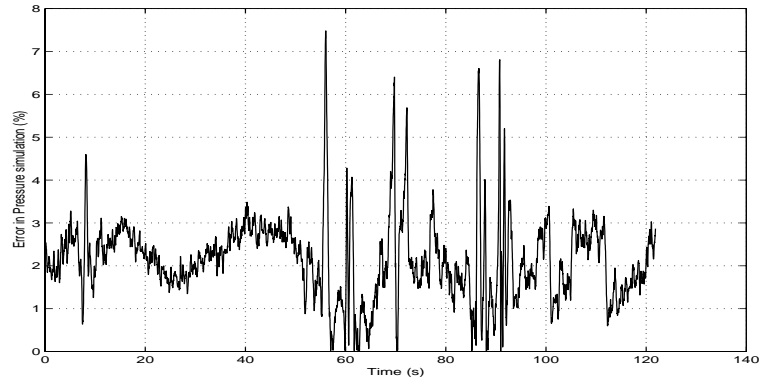
Figure 6.5: Relative error in pressure simulation using the modified engine testbed data map

6.1.3   Map from roll testbed

Since this map is based on measurements collected with the research car it should be the one that best describe the port air mass flow. Judging from figure 6.6 and 6.7 this is also the case.
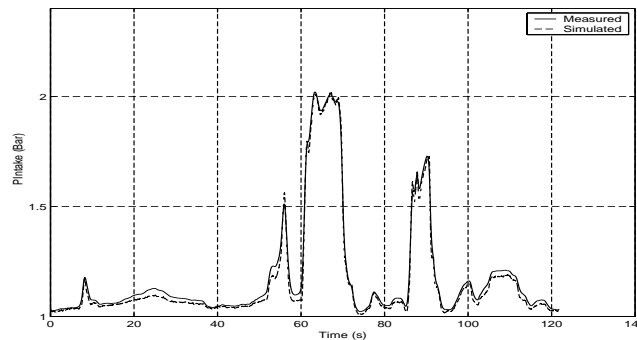
Figure 6.6: Pressure simulation using map based on roll testbed data

6.1.4   Validation summary

In table 6.1 the relative error for the pressure simulations using the different volumetric efficiency maps are shown. As suspected the map based on mea-
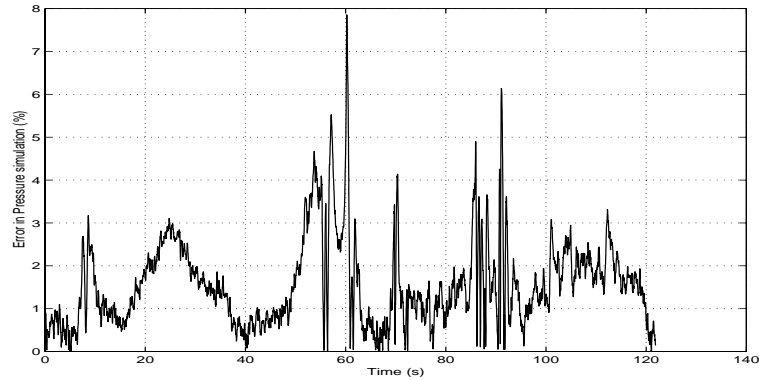
Figure 6.7: Relative error in pressure simulation using map based on roll testbed data

surements from the roll testbed gives the most accurate result. This map will also be used for the validation of the intake manifold models. Using this map has some drawbacks since it does not cover the whole operating range of the engine (see section 5.2). For future work a new and complete volumetric efficiency map should be created so validation can be made over the whole operating range of the engine.

Data source	Relative error (%)
Engine testbed	13,69
Modified engine testbed	2,15
Roll testbed	1,56

Table 6.1: Relative errors for the pressure simulations

6.2   Validation of Intake Manifold Models

The intake manifold models will be validated regarding both pressure and temperature in the manifold, where pressure is the most interesting quantity. This validation is made using measurement data collected from the research car during various driving conditions. The pressure measurement data is collected using both the production line sensor and an extra sensor. The production line sensor is used by the ECU to collect data. It is a standard component that was installed when the car was produced. The extra sensor is part of the additional measurement system described in section 3.4. The average value of the two signals are used as the pressure reference. A uniform temperature in the intake manifold is assumed, the real temperature is however distributed inside the manifold. This makes it hard to get a correct measurement of the temperature since the one measured is only a local value around the sensor.

Also the simulation time of the models is of interest. A model implemented in the ECU for On Board Diagnosis purposes often has to be simulated on-line, and since the computational power of the ECU is limited this means that the model can't be too complex. The intake manifold models are simulated using Matlab/Simulink on a 550 MHz Pentium 3 computer with 256 MB of RAM and Windows 98 operative system.

Two measurement/simulation files are presented in the following sections for each of the different models, one with the EGR system disabled and one with active EGR system. A disabled EGR system means simply that the EGR valve is stuck in a closed position (see figure 2.3). When the EGR system is active the EGR valve is controlled by the ECU. This means that depending on the operating point of the engine the EGR valve is open or closed, which results in rapid changes of the EGR flow. Since the EGR flow has a big influence on both intake manifold pressure and temperature it is important to model this flow accurately.

The engine speed profiles for the two measurement files used for validation is shown in figure 6.8 (without EGR) and 6.9 (with EGR). In figure 6.10 the simulated EGR flow into the manifold is shown. This is for showing where in the simulation the EGR is active.

The error in the simulations are calculated in the following way

$$Error = \frac{|Simulated\ value - Measured\ value|}{Measured\ value}$$

6.2.1 p & m state model

In figure 6.11 and 6.12 the simulation results from the p&m state model are presented. When EGR is inactive (figure 6.11) the pressure simulation follows the measured signal quite well. It is always a bit to low though. In the pressure error plot we can see that the maximum error is about 7,5%. This error occurs when there is a fast pressure change in the manifold. Also other spikes can be seen in the parts of the signal where the pressure is rapidly changing. For the temperature simulation a similar behavior like the pressure simulation can be observed. The simulated temperature is always a bit low, but the main error occurs during rapid dynamic behavior of the system. This behavior of the temperature simulation is expected because the calculation of the temperature is based on the pressure and gas mass inside the manifold (see equation 4.14). And since a change of pressure can occur much faster than a change of temperature, a temperature spike can be produced when the pressure is changing fast.

When EGR is active (figure 6.12) a much larger error can be seen in both the pressure and temperature simulation. An error of up to 50% in the pressure simulation and 60% in the temperature simulation indicates a poor EGR model.

6.2.2 p & T state model

The validation for this model without EGR is presented in figure 6.13. The pressure simulation is very similar to the one with the p&m state model, and hence the relative error is almost the same. This is expected since the only difference in the two pressure state equations is that the gas properties are treated differently (see equations 4.11 and 4.21). In the temperature simulation however a major improvement can be seen. All of the spikes shown in the previous simulation are gone and the simulated signal follows the measured very accurately. The simulated temperature does not quite come up to the temperature measurements however. This is thought to be a result of heat transfer in the intake manifold. The location of the temperature sensor may also be important.

When EGR is active (figure 6.14) there are again large errors in the simulations. An improvement from the p&m state model can be seen in the absence of too large and fast changes in both simulated pressure and temperature.

6.2.3   p & T state model including heat transfer

The simulation results for this model without EGR can be seen in figure 6.15. The temperature simulation shows the most improvements but also the pressure is slightly improved.

With EGR active (figure 6.16) we can now see that the temperature signal looks much better than with the two previous models. There is still a large maximum error of about 30% but the overall error is smaller and it shows that the simulation follows the measurement quite well.

A problem occurs when heat transfer is included in the state equations. This problem is that the intake manifold wall temperature (T_{Wall}) in equation (4.27) has to be known. There is no sensor for this temperature so only a rough approximation has been used. The approximation consists of taking the ambient temperature (T_{Amb}, which is measured) and adding a certain temperature to this one depending on the temperature and operating point of the engine. How this is implemented in Simulink can be seen in figure B.3 and B.4 in appendix B. In this thesis the temperature increase has been added manually which of course has the disadvantage of not being able to change during a simulation. For future work it would be interesting to investigate the intake manifold wall temperature, for example by applying a temperature sensor and see if this temperature can be approximated by some other temperature already measured in the engine. Also the heat transfer coefficient (h_{HT}) in equation (4.27) has to be known. It is set to a value of $25W/K$ which is suggested in [13]. Based on the simulations performed here this value has a good accuracy for this manifold. A more detailed study regarding the heat transfer might be interesting for future work.

6.2.4   Validation summary

In tables 6.2 and 6.3 the relative errors and the simulation time of the different models are presented. Six measurement files are used for the validation without EGR and three when the EGR system is active. The measurement files used for generating the simulation results in figures 6.11-6.16 are number 2 (without EGR) and number 7 (with EGR). Figures representing the other simulations can be found in appendix A.

In table 6.2 (without EGR) we can see that the error in the pressure simulation is quite similar between the three models. As stated before this is expected since the pressure is modeled in a very similar way. What can be concluded of this however is that the assumption of equal air and exhaust

gas properties (made in the models based on pressure and temperature) does not lessen the accuracy of the simulation to any large extent. The error in the temperature simulation is quite similar between the p&m,- and p&T-state model. In simulations with these models often what looks like an offset error can be seen in the temperature. One reason is probably heat transfer in the manifold which is not included in the model. When this heat transfer is included we can see that the temperature error in the simulations decreases to a large extent. Thus, heat transfer seems to be important to consider when modeling the intake manifold. Not only because the temperature prediction is more accurate, but also the pressure prediction since it depends on the temperature in the manifold. The simulation time of the models based on p&T is several times smaller than of the model based on p&m. This is valuable since the goal is to create models that are computationally simple. The reduction in simulation time is most likely due to more simple equations.

In table 6.3 the results from simulations with an active EGR system is presented. We can see that the pressure simulation is somewhat better in the models based on p&T. The errors are overall quite large though and must be reduced before these models can be of any practical use. In the temperature simulations the model including heat transfer is again the most accurate, though errors are present in all models here as well.
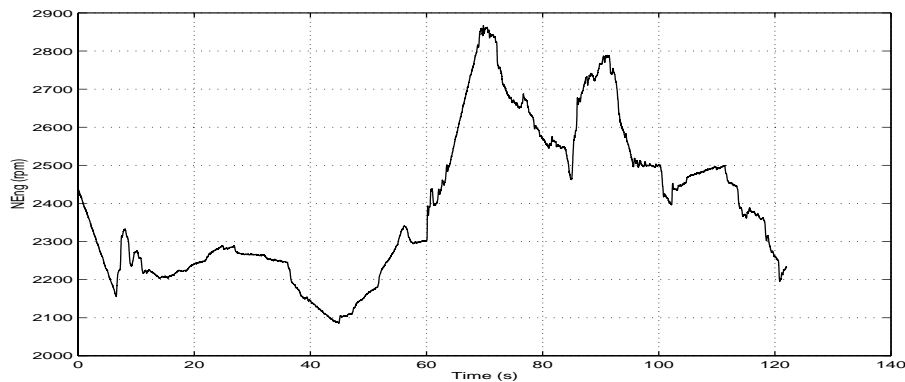
Figure 6.8: Engine speed profile for validation without EGR
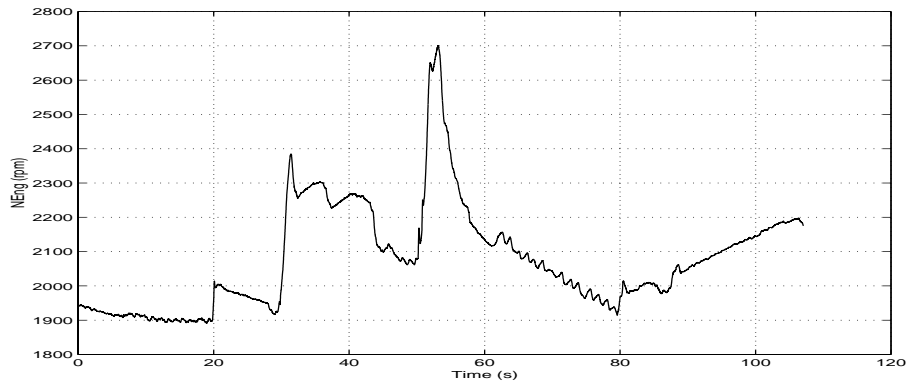
Figure 6.9: Engine speed profile for validation with EGR
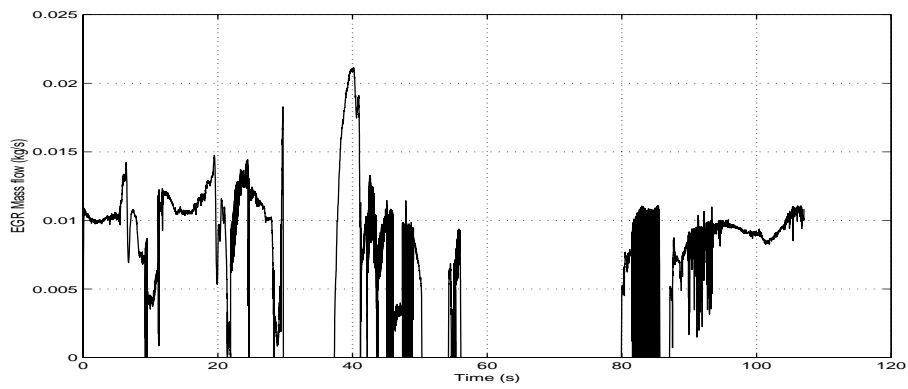
Figure 6.10: EGR flow into manifold for validation files

		Simulation number					
		1	2	3	4	5	6
$p\&m$-	p_{Error} [%]	1.45	1.57	2.79	1.24	1.46	1.23
state-	T_{Error} [%]	7.60	7.59	10.30	7.12	6.70	3.32
model	T_{Sim} [s]	26.5	24.0	11.0	22.1	10.8	20.5
$p\&T$-	p_{Error} [%]	1.48	1.68	2.92	1.60	1.46	1.34
state-	T_{Error} [%]	7.77	6.12	9.29	3.96	6.40	1.63
model	T_{Sim} [s]	6.9	5.7	3.0	5.2	2.9	6.7
$p\&T$-	p_{Error} [%]	0.92	1.27	2.54	1.53	1.08	1.37
state-	T_{Error} [%]	5.84	4.53	1.83	1.81	3.11	1.18
model+HT	T_{Sim} [s]	7.0	6.3	3.2	5.5	3.0	6.8

Table 6.2: Relative errors and simulation time of the different models when EGR is not active

		Simulation number		
		7	8	9
$p\&m$-	p_{Error} [%]	6.61	5.77	3.54
state-	T_{Error} [%]	12.89	12.74	19.00
model	T_{Sim} [s]	20.2	39.2	22.3
$p\&T$-	p_{Error} [%]	4.10	4.87	3.38
state-	T_{Error} [%]	12.84	13.04	17.40
model	T_{Sim} [s]	27.0	20.5	28.0
$p\&T$-	p_{Error} [%]	4.28	4.59	3.32
state-	T_{Error} [%]	8.48	8.58	8.59
model+HT	T_{Sim} [s]	27.2	22.1	28.1

Table 6.3: Relative errors and simulation time of the different models when EGR is active
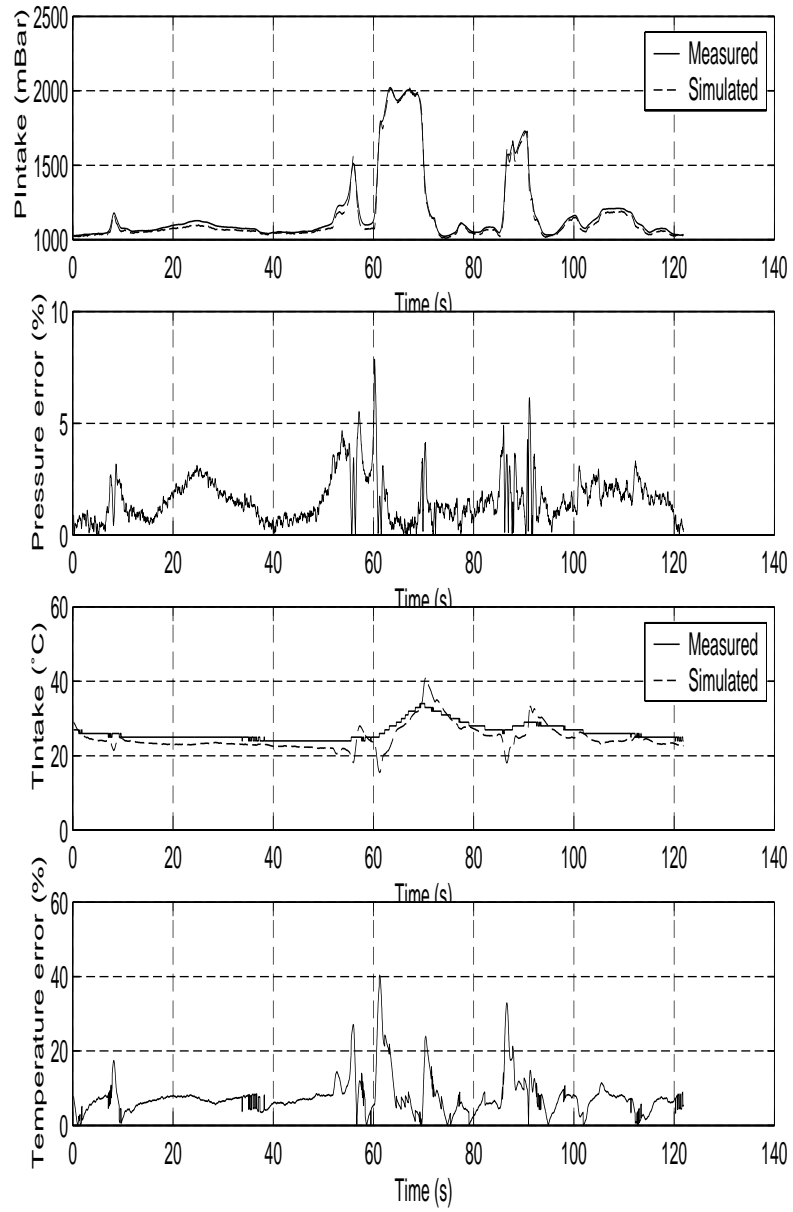
Figure 6.11: Comparison between the p&m state model and measurements. EGR is not active.
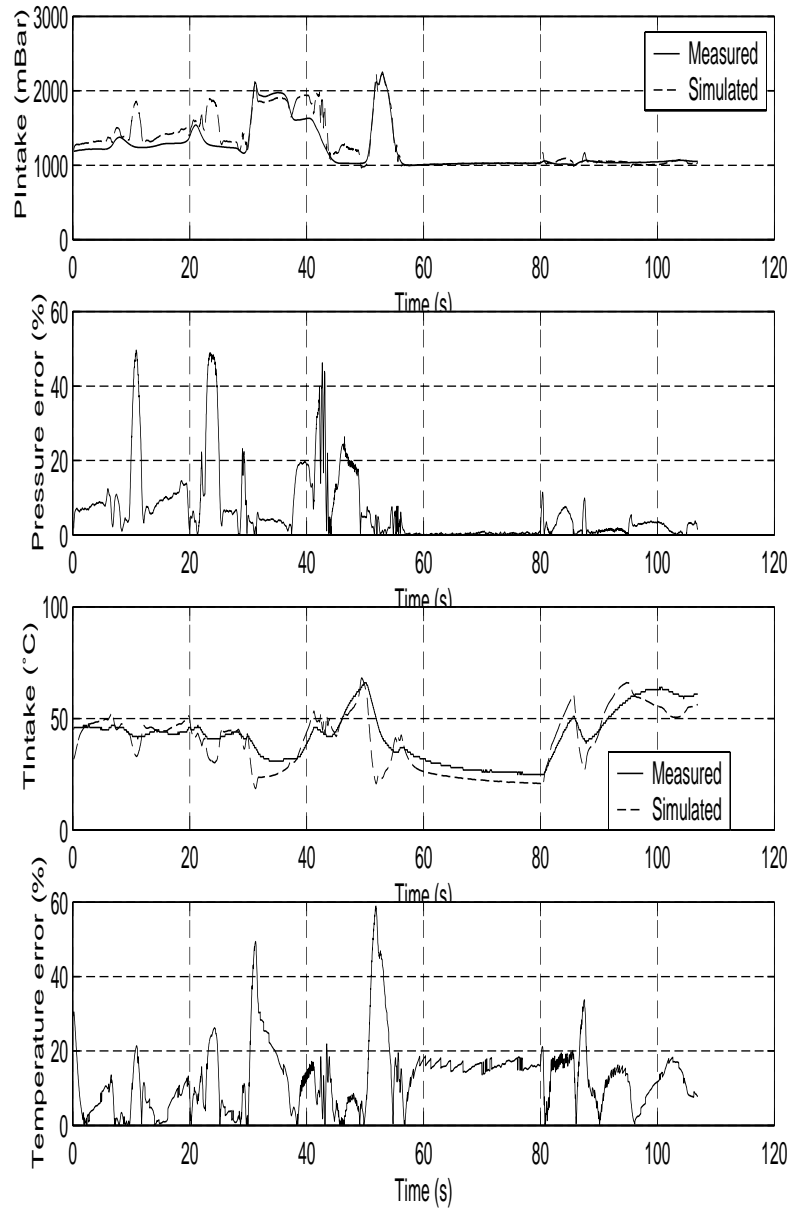
Figure 6.12: Comparison between the p&m state model and measurements. EGR is active.
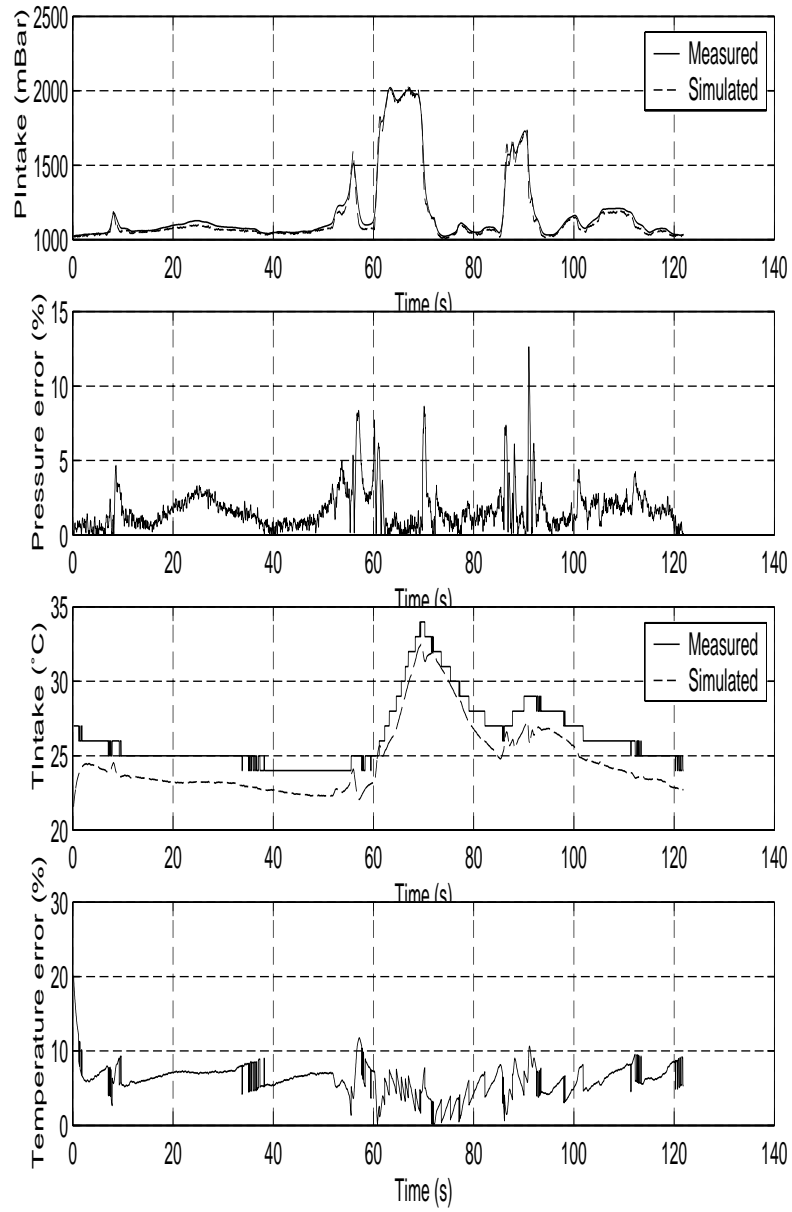
Figure 6.13: Comparison between the p&T state model and measurements. EGR is not active.
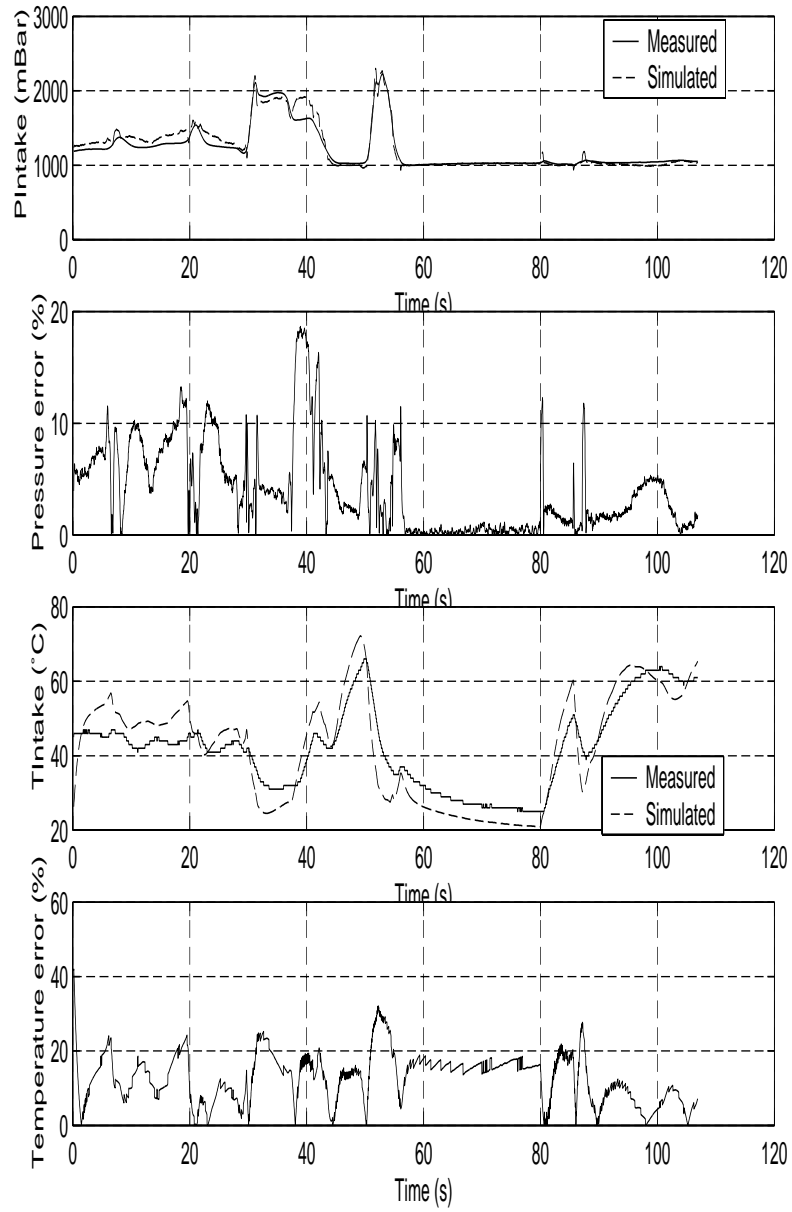
Figure 6.14: Comparison between the p&T state model and measurements. EGR is active.
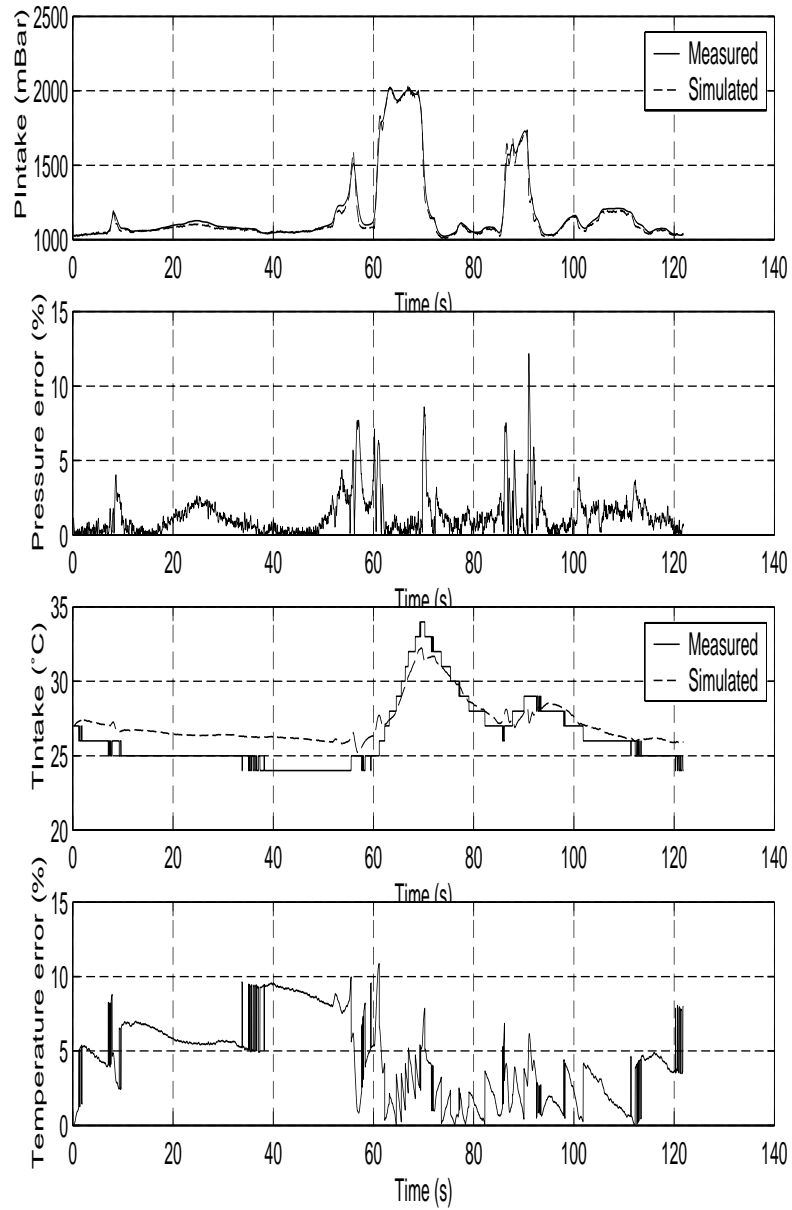
Figure 6.15: Comparison between the p&T state model including heat transfer and measurements. EGR is not active.
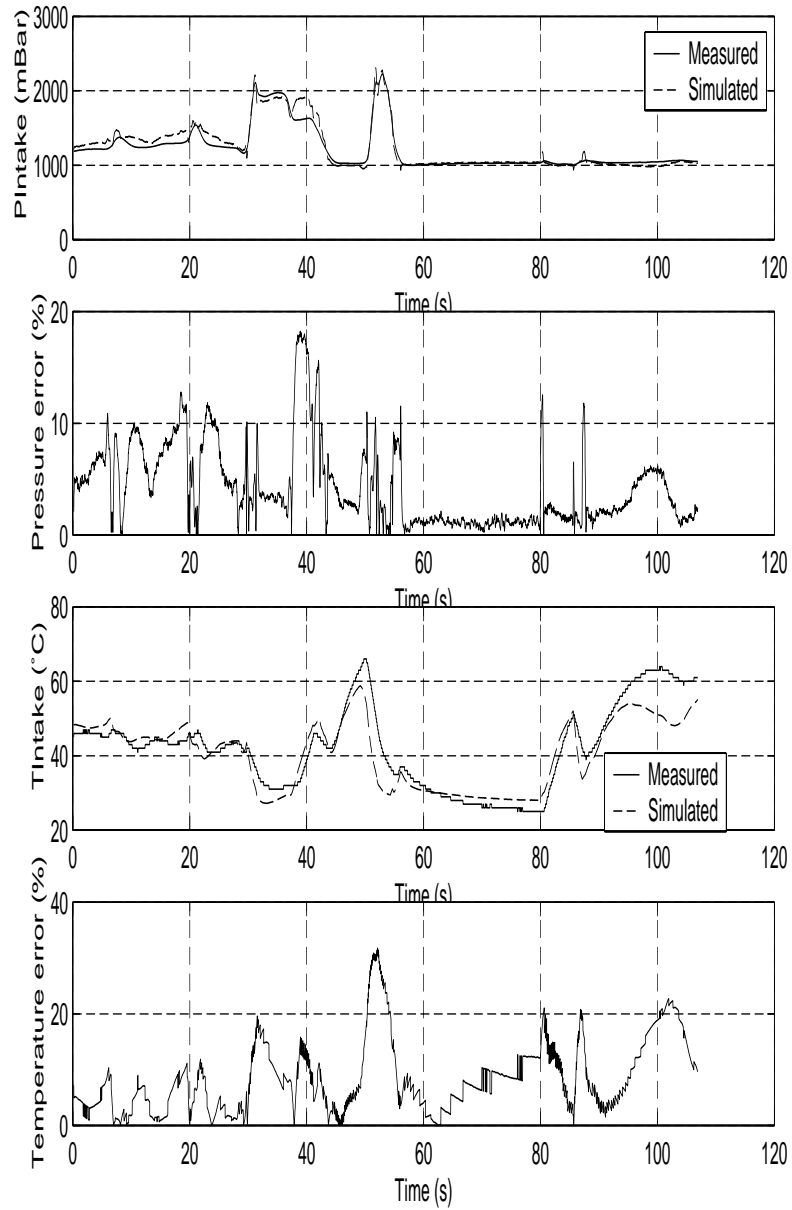
Figure 6.16: Comparison between the p&T state model including heat transfer and measurements. EGR is active.

7 Extensions

For future work the effect of heat transfer in the manifold would be interesting to investigate further. For making the model including heat transfer of practical use, the intake manifold wall temperature has to be found, either by simply measuring it or creating a model for it. Also the accuracy of the heat transfer coefficient should be validated.

Since the models work poorly when the EGR system is active it has to be investigated whether the modelling of the EGR system is correct. This is a good base for a future project.

A new and complete volumetric efficiency map should be created since the ones existing for this engine are either incorrect or incomplete.

8   Conclusions

Two new dynamic models has been constructed for the intake manifold of a turbocharged diesel engine. One with an adiabatic assumption and one including heat transfer in the manifold. Both models include EGR and are based on physical considerations. Validation of these models with measurement data shows promising results, especially the model including heat transfer.

Comparisons between the newly constructed models, based on pressure and temperature, and the previously developed model, based on pressure and mass, shows that some improvements are made. The temperature spikes present in the simulations with the p&m state model can not be seen in the simulations with the new models. In simulations with the model including heat transfer a large improvement of the temperature signal can be seen, so heat transfer in the manifold is clearly important for accurate modelling of this kind of engine.

When EGR is inactive the error in the pressure simulation does not vary much between the models, when it is active however the models based on pressure and temperature capture the pressure dynamics in a better way. In these models we assume that air and exhaust gas properties are equal. From this the conclusion that the air and exhaust gas properties can be assumed equal when deriving the model equations are drawn. The very short spikes that can be seen in particularly the pressure error plots present no problems since they can easily be filtered away.

For all models errors in both pressure and temperature simulations occurs when EGR is active. This is thought to be due to an erroneous EGR model.

The simulation time of the models are also considered. When EGR is inactive the simulation time of the models based on pressure and temperature are greatly reduced from that of the model based on pressure and mass. This is due to more simple equations. When EGR is active however, no certain conclusions can be drawn from the few simulations presented here.

References

[1] John B. Heywood. *Internal Combustion Engine Fundamentals*. Automotive Technology Series. McGraw-Hill, 1988.

[2] N. Watson and M. S. Janota. *Turbocharging the Internal Combustion Engine*. MacMillan Press Ltd, 1982.

[3] Lars Nielsen and Lars Eriksson. Course material vehicular systems. Linköping Institute of Technology, Vehicular Systems, ISY, 1999.

[4] World Wide Web, http://www.etas.de. Information about ETAS GmbH.

[5] World Wide Web, http://www.ricardo.com. Information about Ricardo Consulting Eng. Ltd.

[6] World Wide Web, http://www.daimlerchrysler.com. Information about Daimler Chrysler AG.

[7] A.J. Truscott. Dynamic diesel engine system for fault detection, theory of model, dp 99/2667. Ricardo Cons. Eng. Ltd., UIX, December 1999.

[8] Nyberg, Stutte, and Wilhelmi. Model based diagnosis of the air path of an automotive diesel engine. IFAC Workshop: Advances in Automotive Control, Kalsruhe, March 2001.

[9] Minghui Kao and John J. Moskwa. Turbocharged diesel engine modeling for nonlinear engine control and state estimation. *Journal of Dynamic Systems, Measurement and Control. Vol. 117, 1995.*

[10] Elbert Hendricks, Alain Chevalier, Michael Fons, Spencer C. Sorenson, Martin Müller, and Christian Vigild. Mean value engine modelling of an si engine with egr. *SAE paper No. 1999-01-0909, 1999.*

[11] Dr. Mattias Nyberg. Thermodynamics of gas volumes and gas mixing. Internal 'Methodentag FT2/EA' at DaimlerChrysler, April 2000.

[12] Elbert Hendricks, Alain Chevalier, Michael Jensen, Spencer C. Sorenson, Dave Trumpy, and Joe Asik. Modelling of the intake manifold filling dynamics. *SAE paper No. 960037, 1996.*

[13] Alain Chevalier, Martin Müller, and Elbert Hendricks. On the validity of mean value engine models during transient operation. *SAE paper No. 2000-01-1261, 2000.*

Appendix A: Simulation results

In this section the simulation results for the measurement files not presented in the validation chapter are shown.
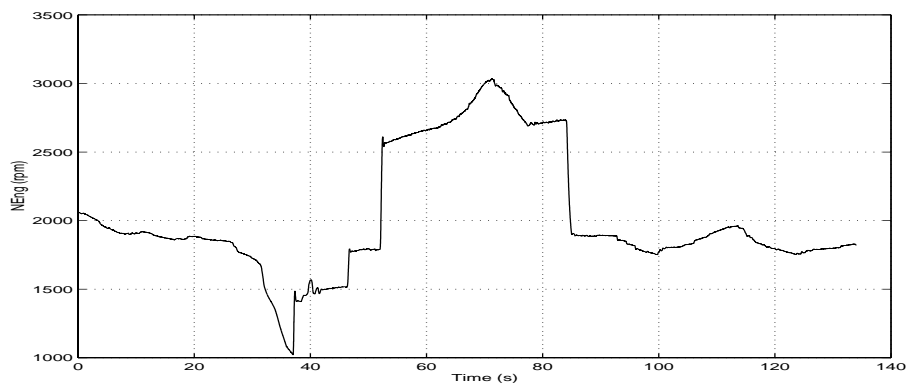
Figure A.1: Engine speed profile for simulation file 1.
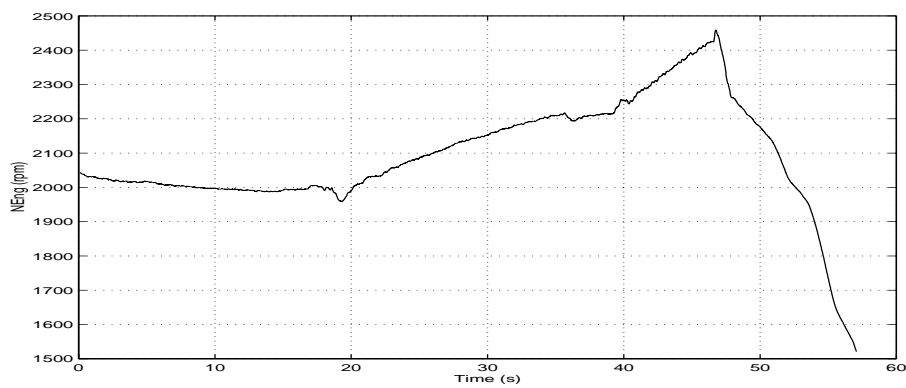
Figure A.2: Engine speed profile for simulation file 3.
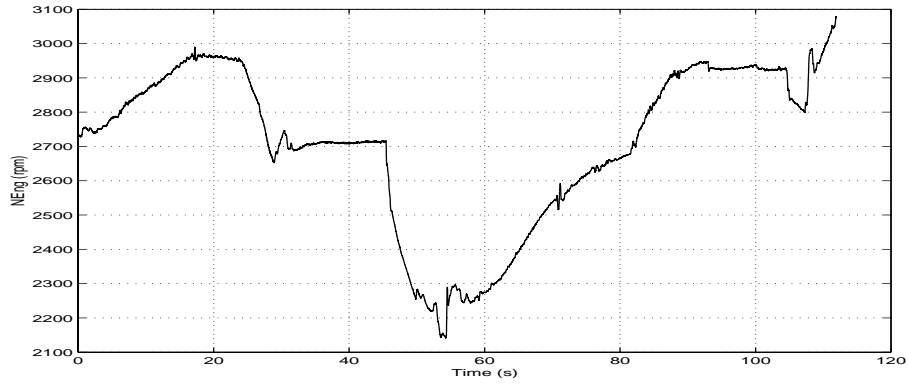
Figure A.3: Engine speed profile for simulation file 4.
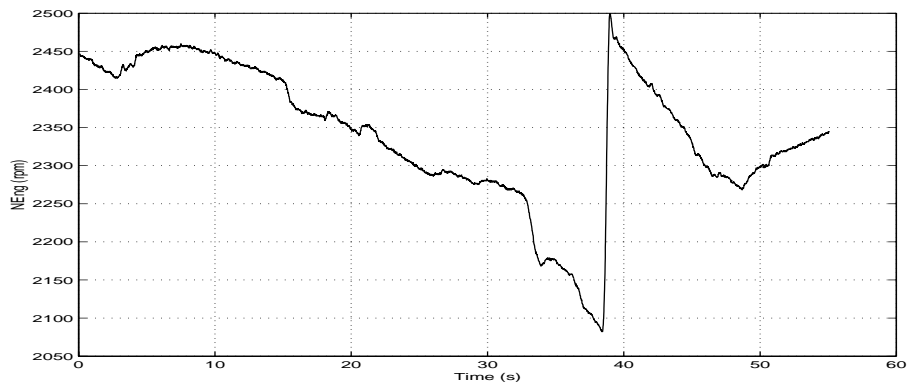
Figure A.4: Engine speed profile for simulation file 5.
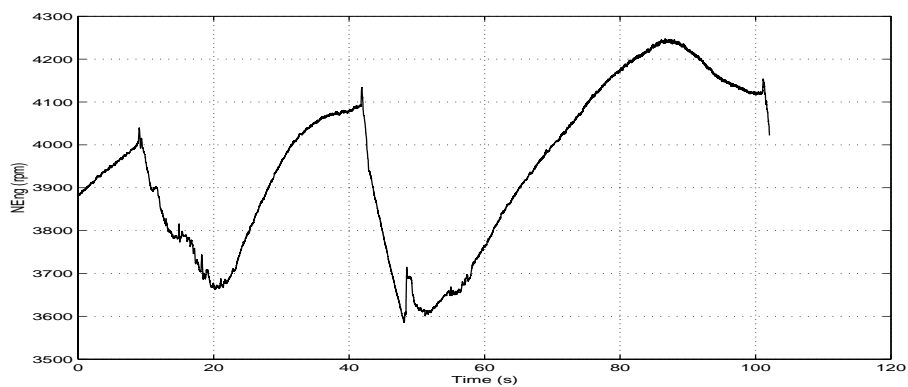
Figure A.5: Engine speed profile for simulation file 6.
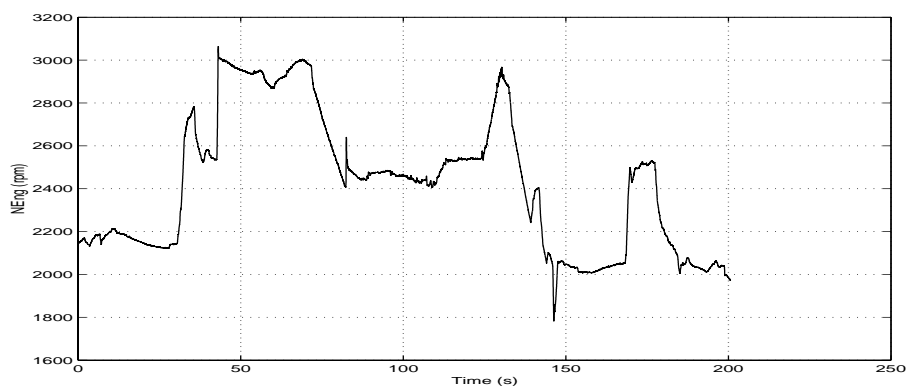
Figure A.6: Engine speed profile for simulation file 8.
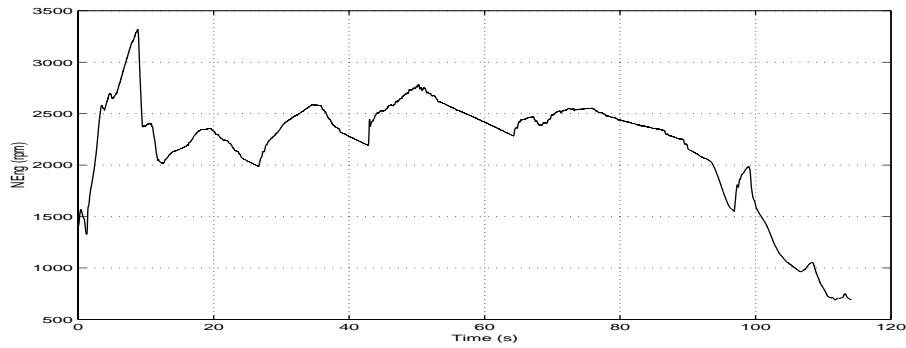
Figure A.7: Engine speed profile for simulation file 9.
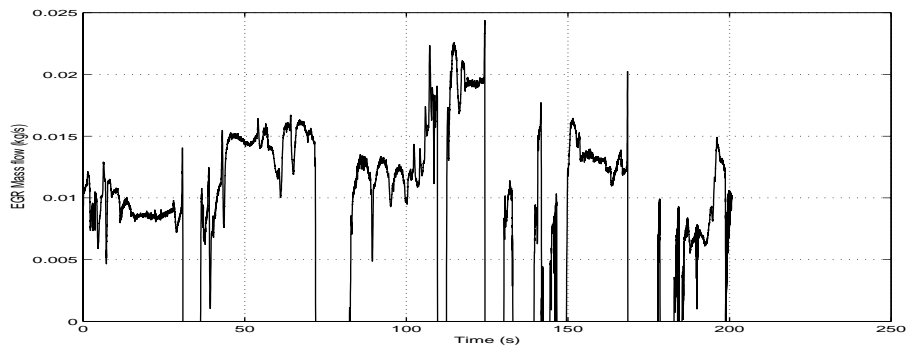
Figure A.8: Simulated EGR flow into manifold for simulation file 8.
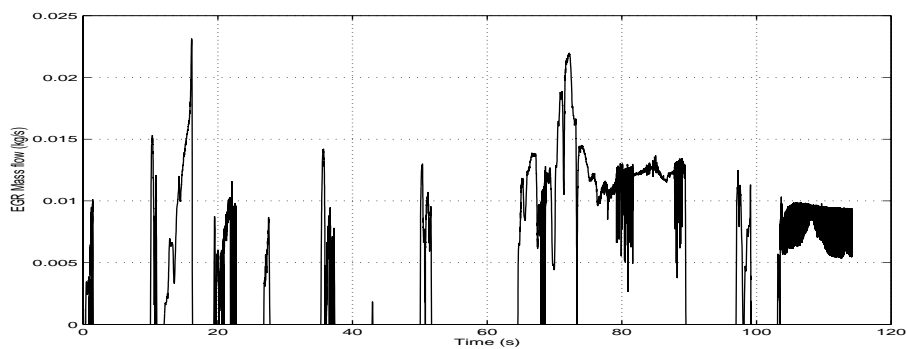
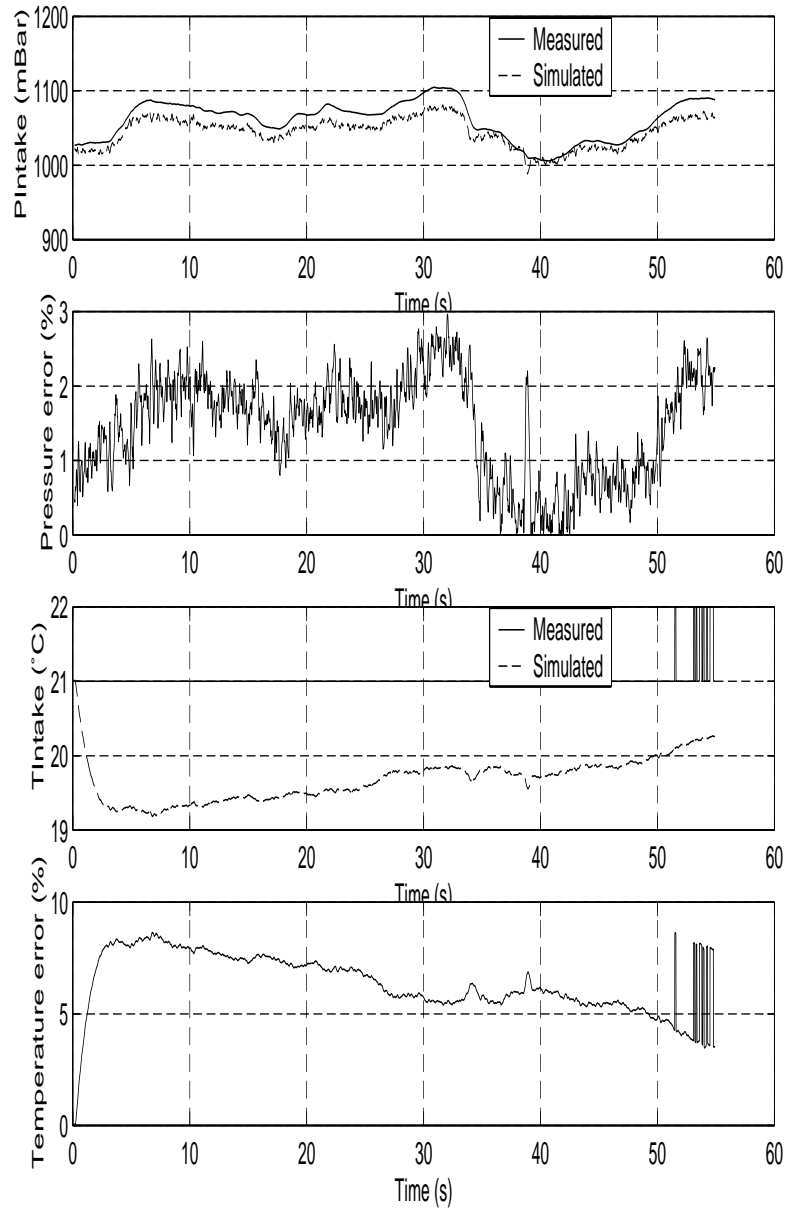Figure A.9: Simulated EGR flow into manifold for simulation file 9.
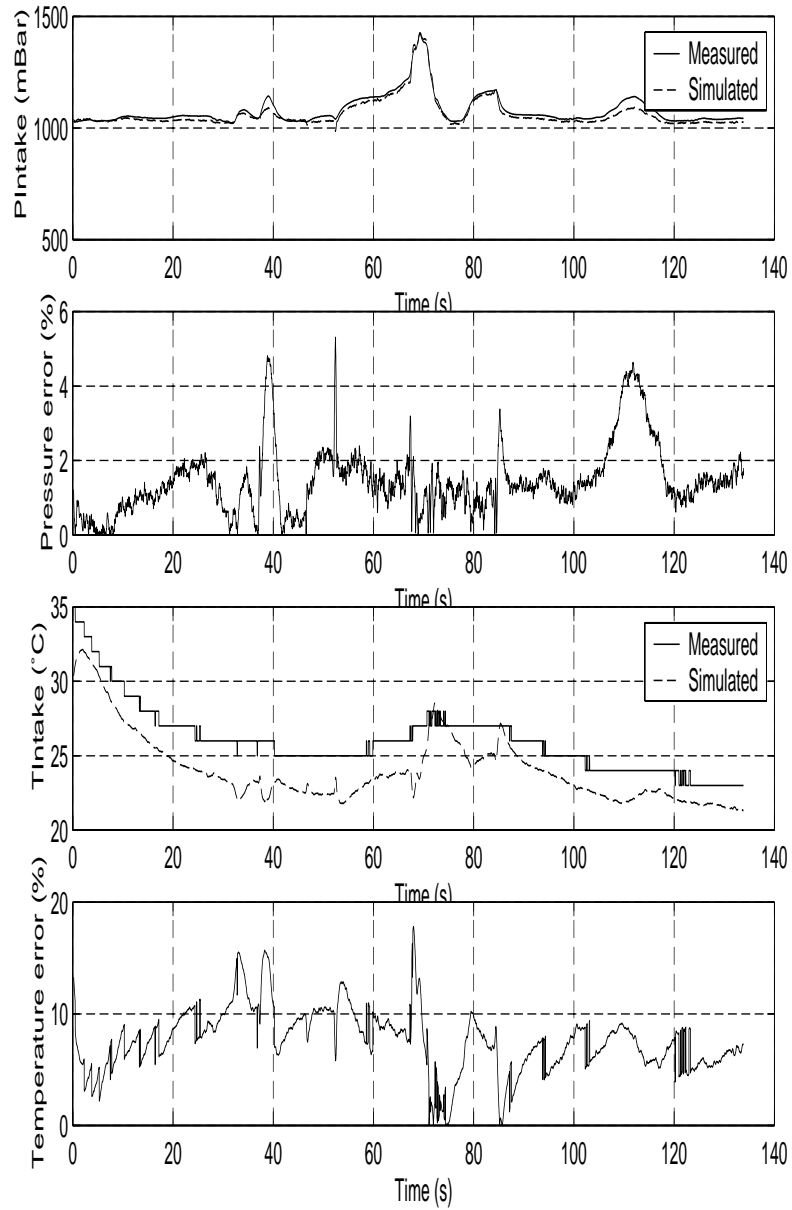
Figure A.10: Comparison between the p&m state model and measurements when EGR is not active. Simulation file 1.
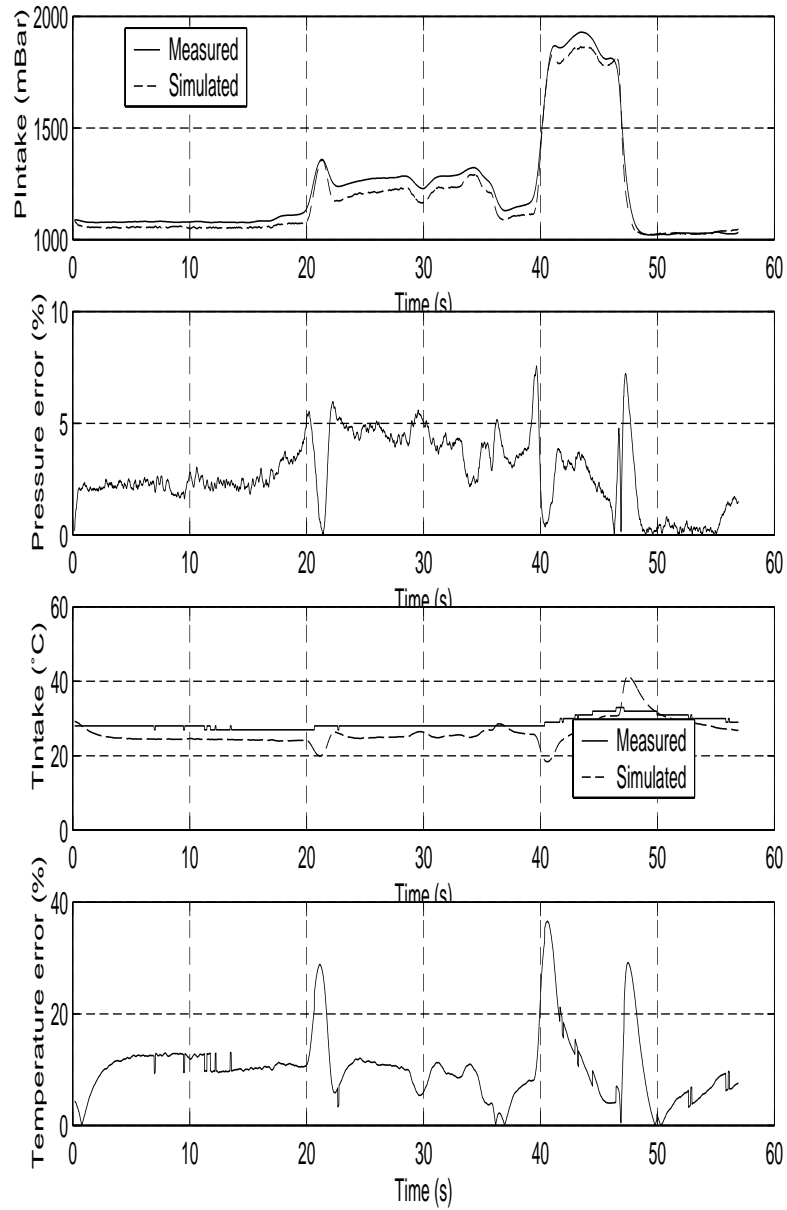
Figure A.11: Comparison between the p&m state model and measurements when EGR is not active. Simulation file 3.
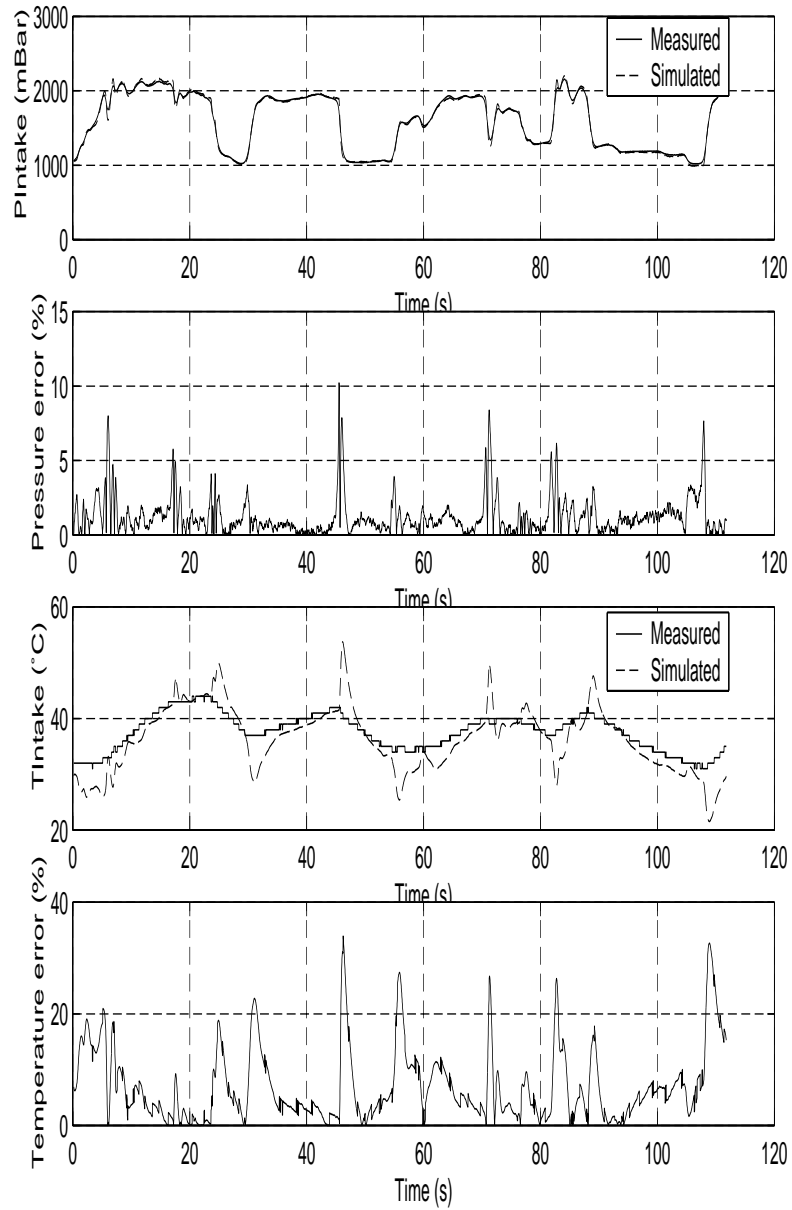
Figure A.12: Comparison between the p&m state model and measurements when EGR is not active. Simulation file 4.
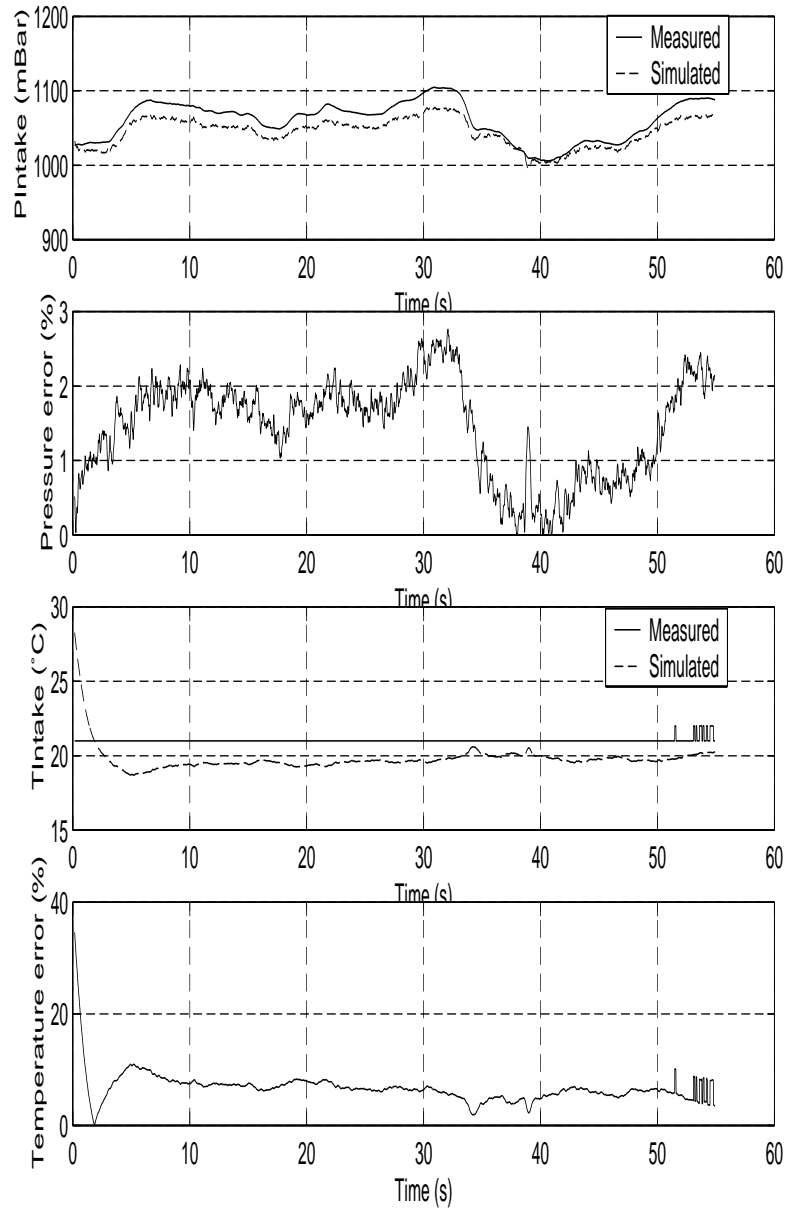
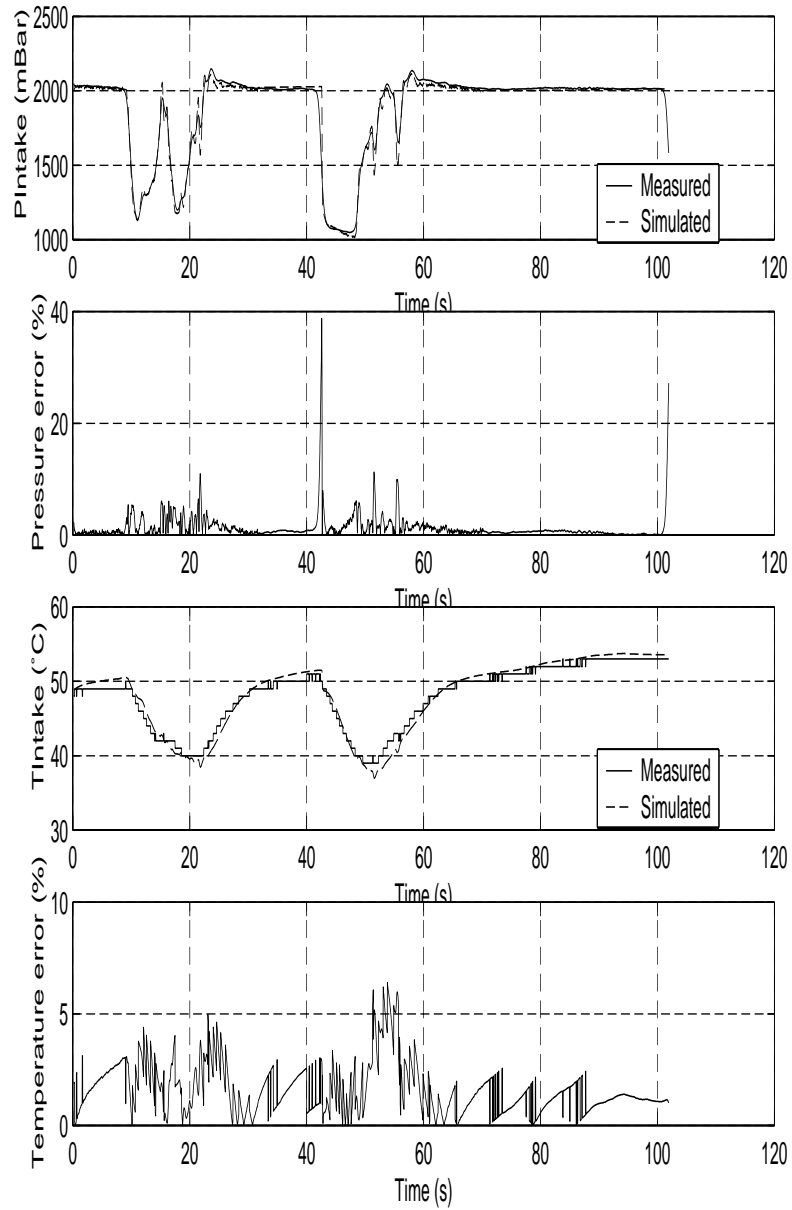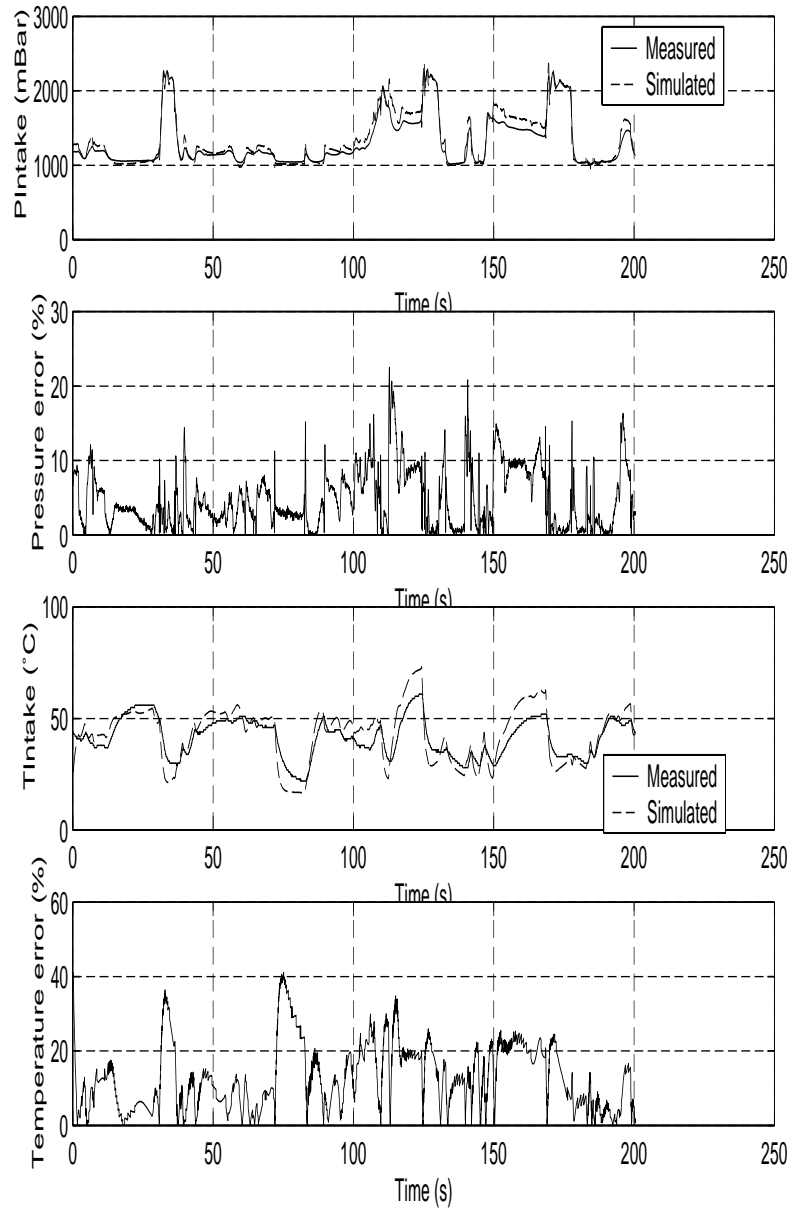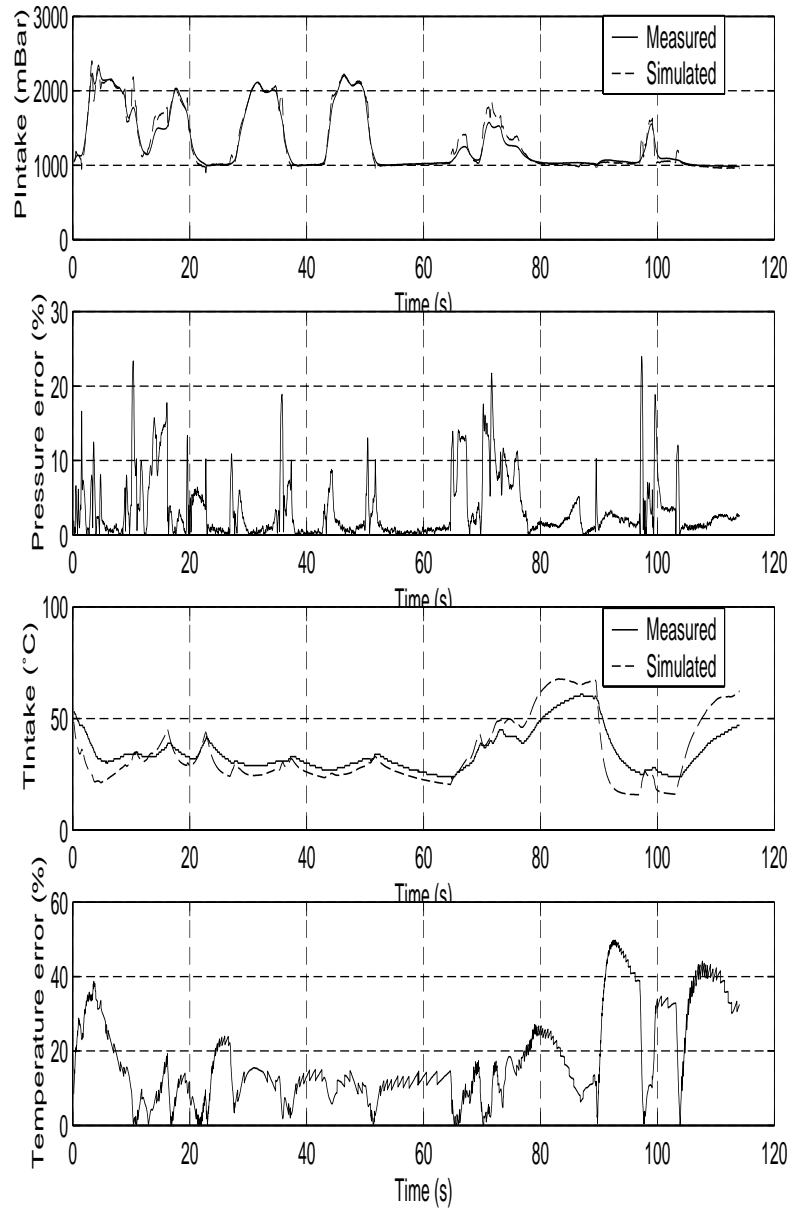Figure A.13: Comparison between the p&m state model and measurements when EGR is not active. Simulation file 5.
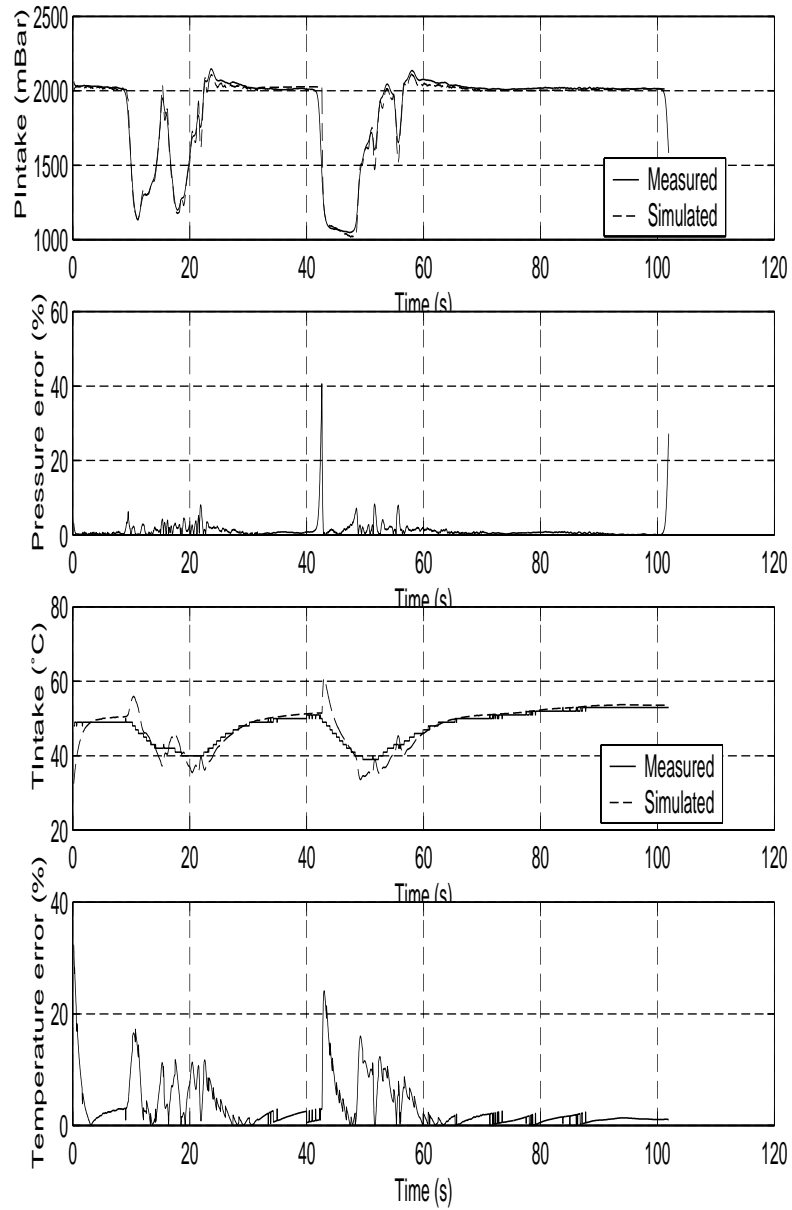
Figure A.14: Comparison between the p&m state model and measurements when EGR is not active. Simulation file 6.
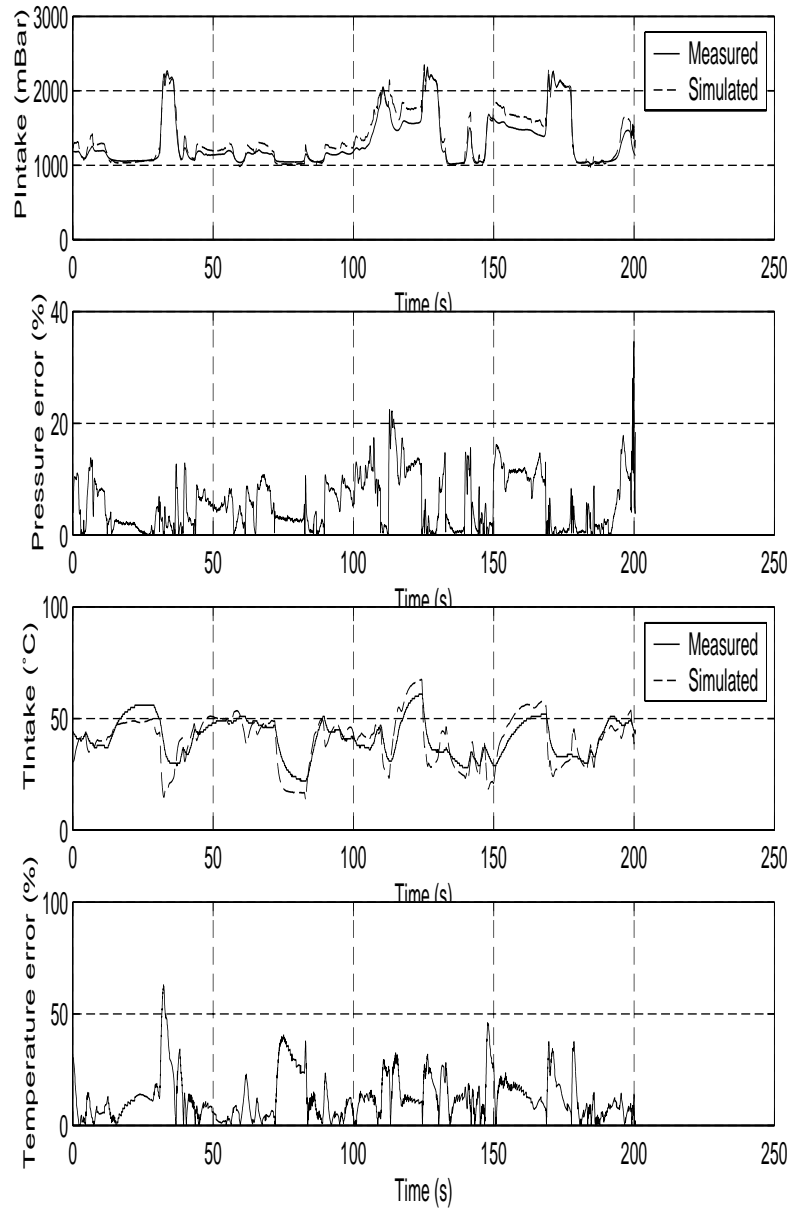
Figure A.15: Comparison between the p&m state model and measurements when EGR is active. Simulation file 8.
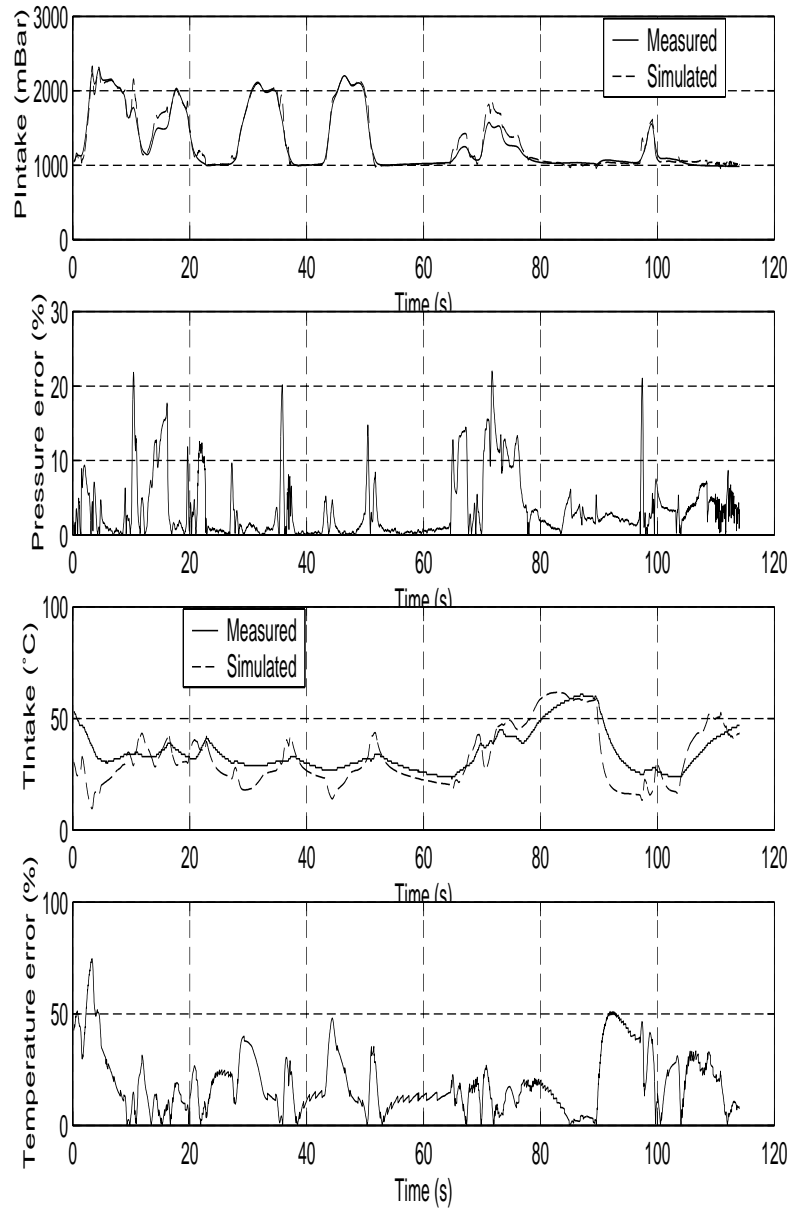
Figure A.16: Comparison between the p&m state model and measurements when EGR is active. Simulation file 9.
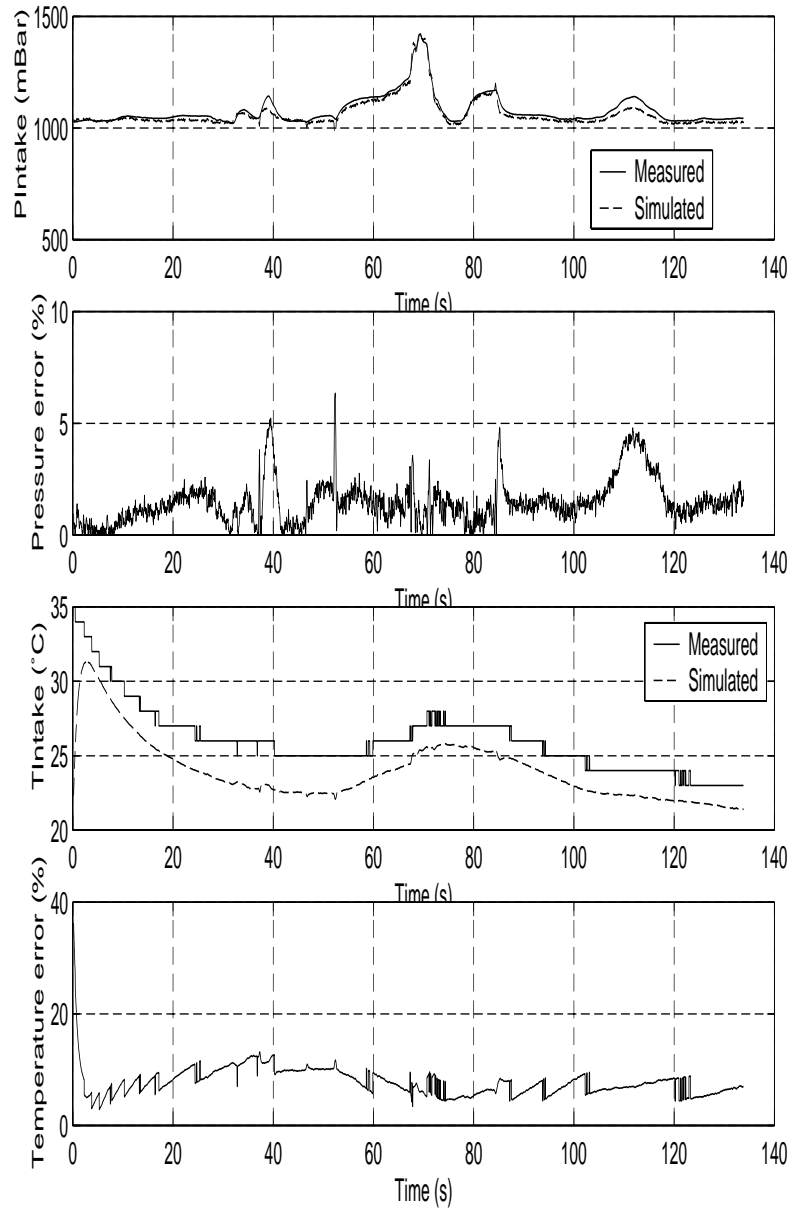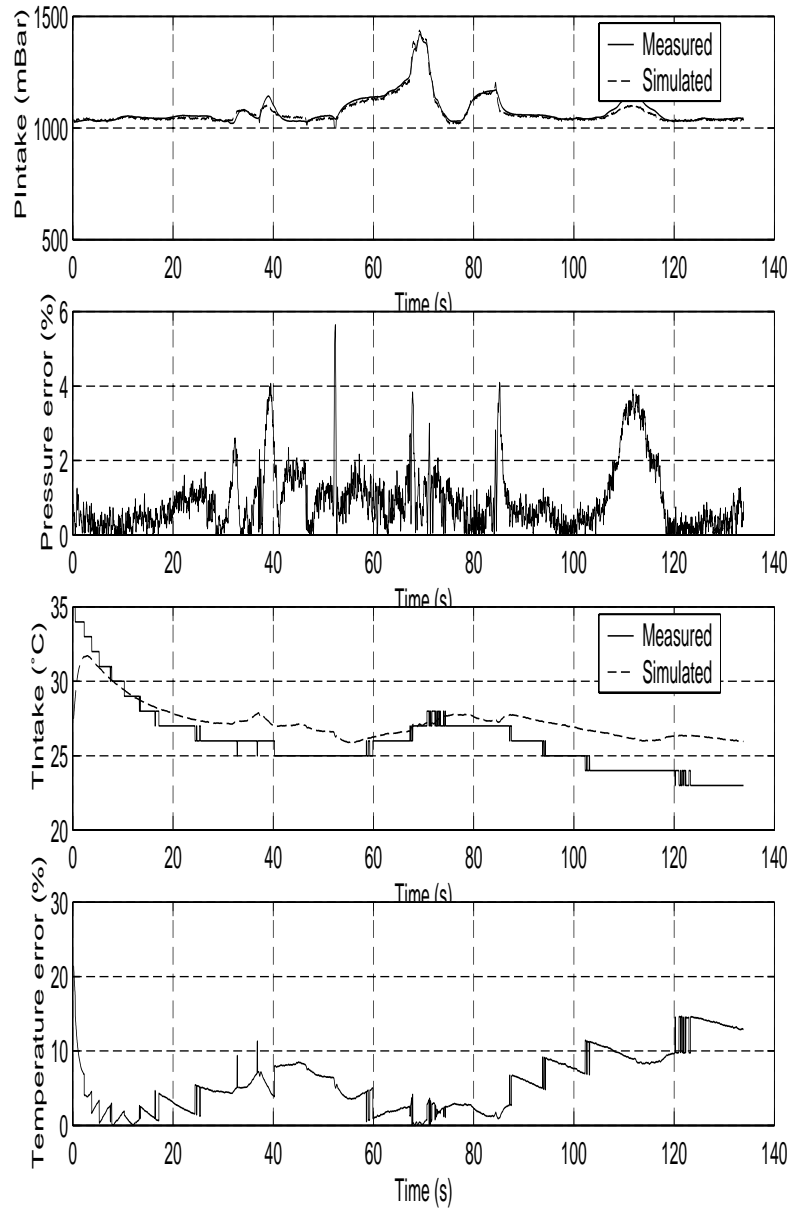
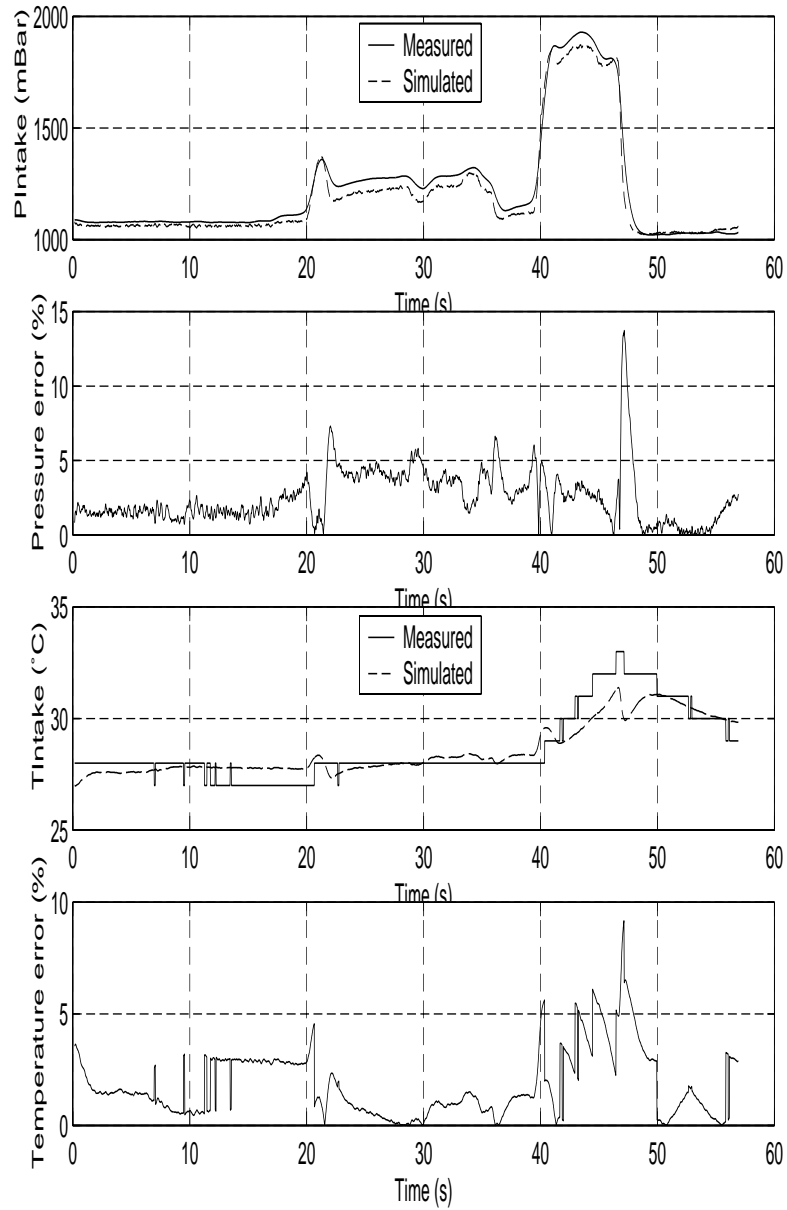Figure A.17: Comparison between the p&T state model and measurements when EGR is not active. Simulation file 1.
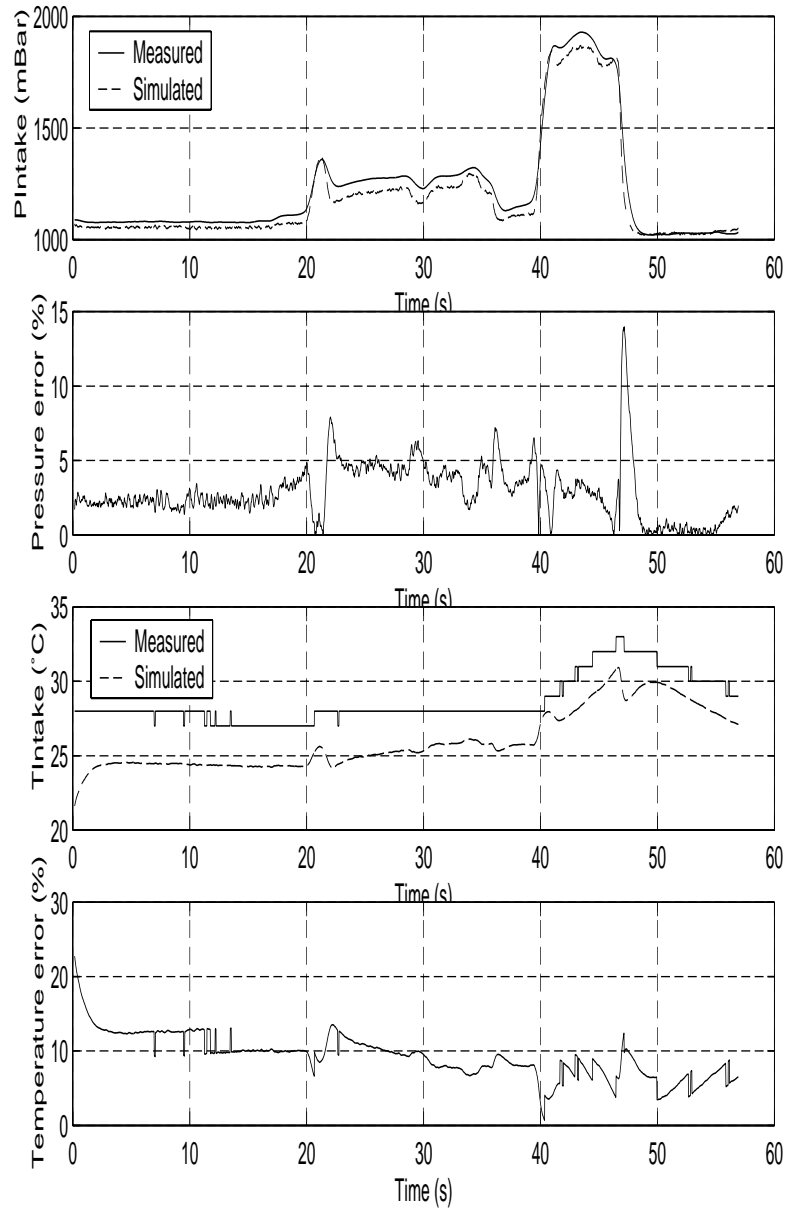
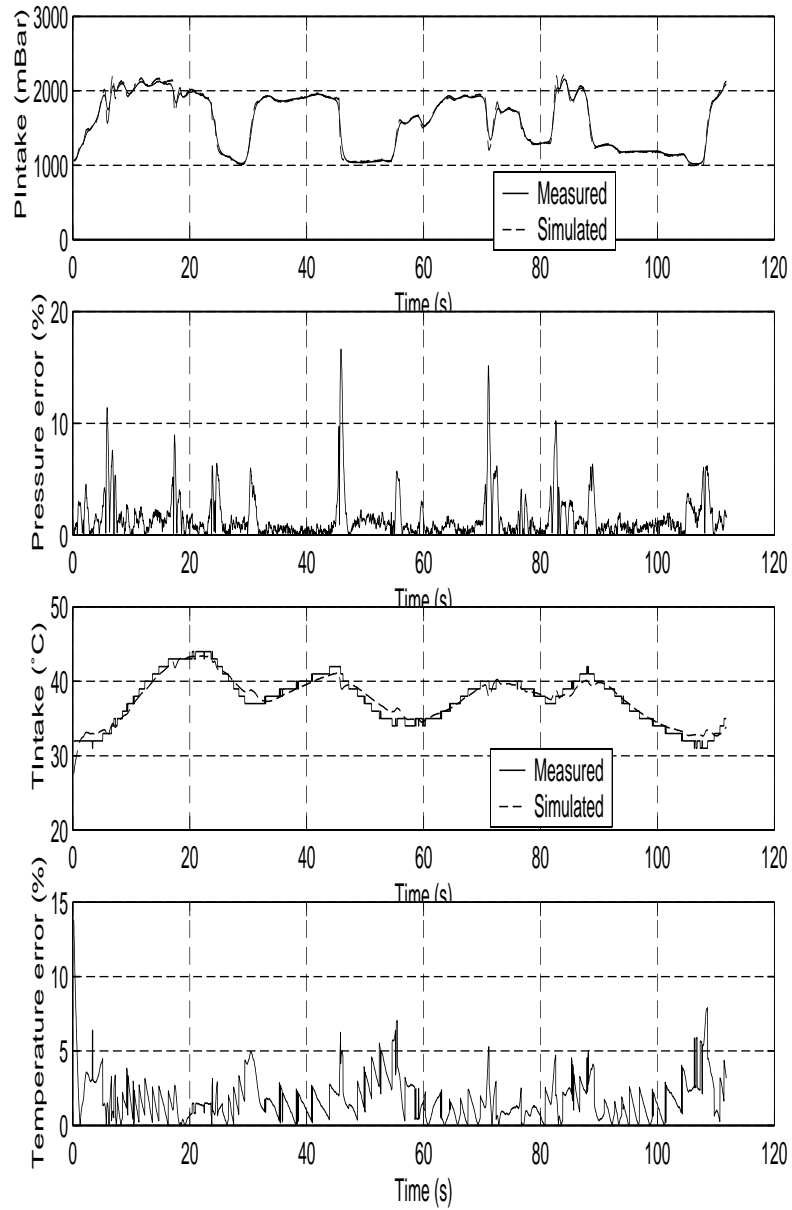Figure A.18: Comparison between the p&T state model and measurements when EGR is not active. Simulation file 3.
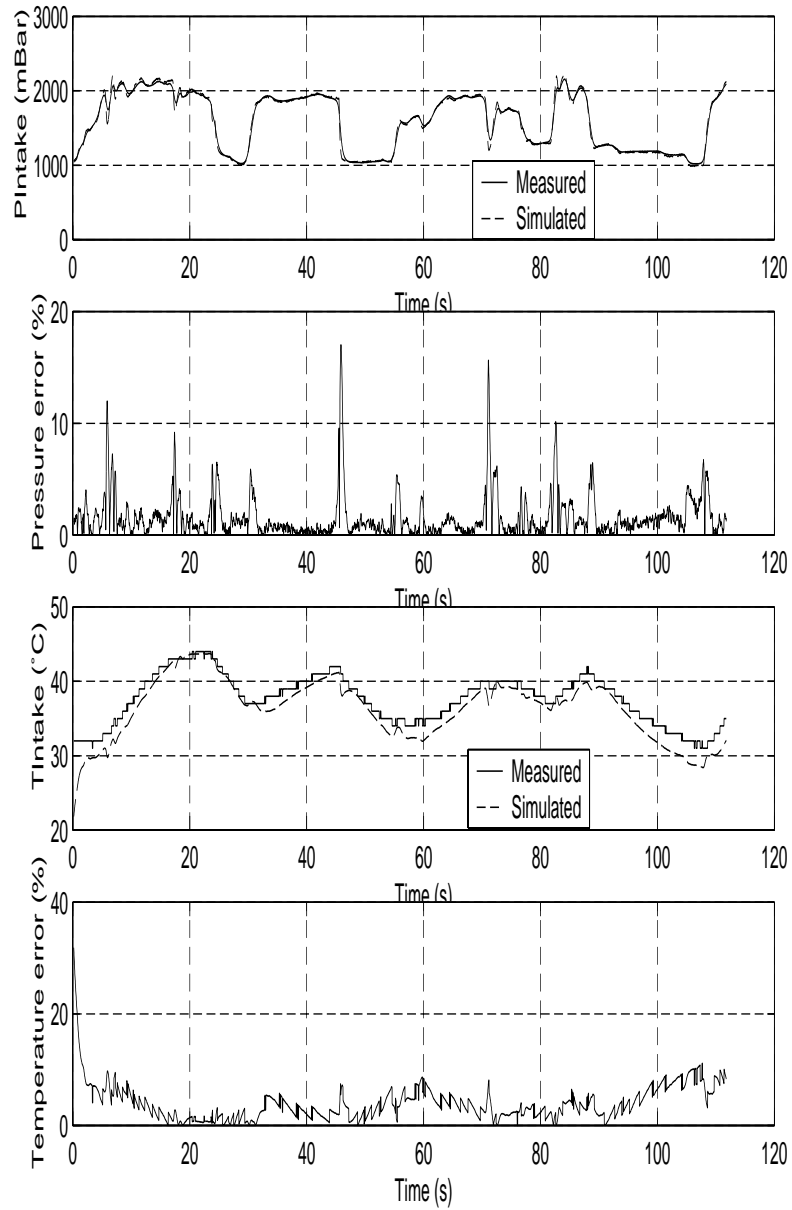
Figure A.19: Comparison between the p&T state model and measurements when EGR is not active. Simulation file 4.

Figure A.20: Comparison between the p&T state model and measurements when EGR is not active. Simulation file 5.

Figure A.21: Comparison between the p&T state model and measurements when EGR is not active. Simulation file 6.

Figure A.22: Comparison between the p&T state model and measurements when EGR is active. Simulation file 8.

Figure A.23: Comparison between the p&T state model and measurements when EGR is active. Simulation file 9.
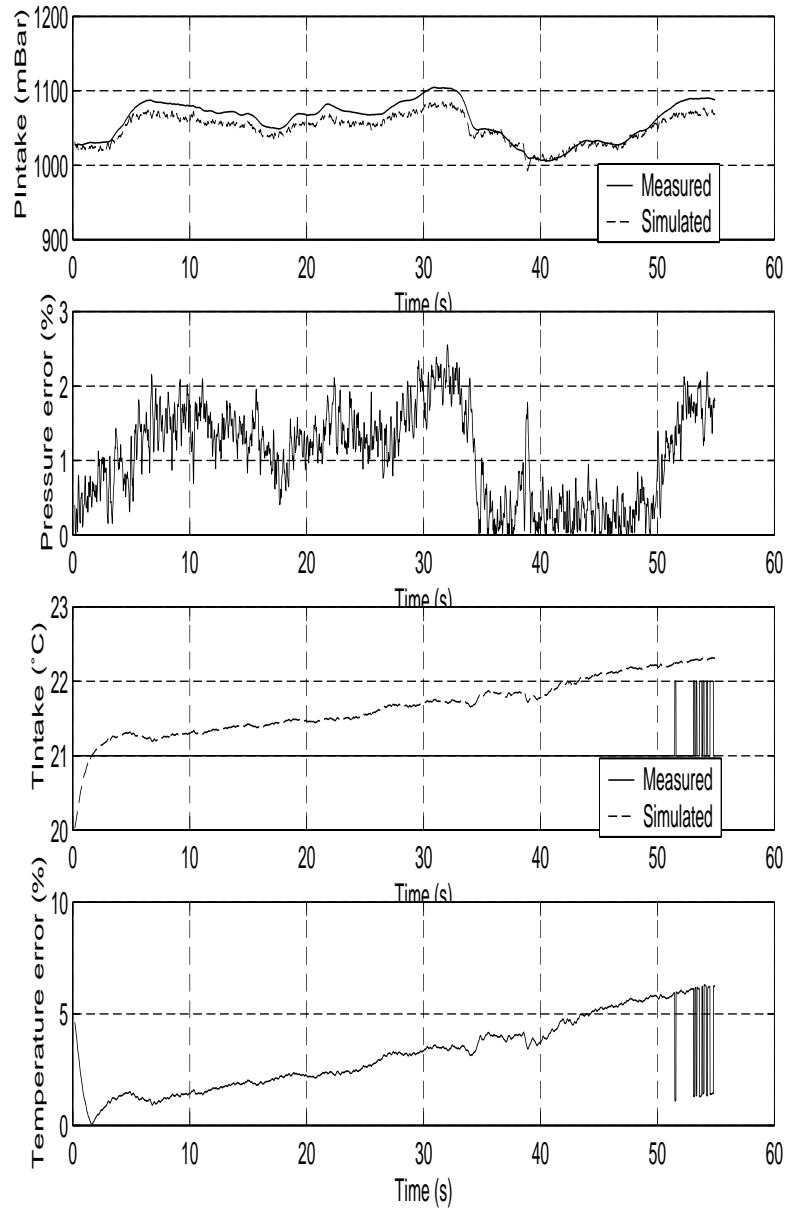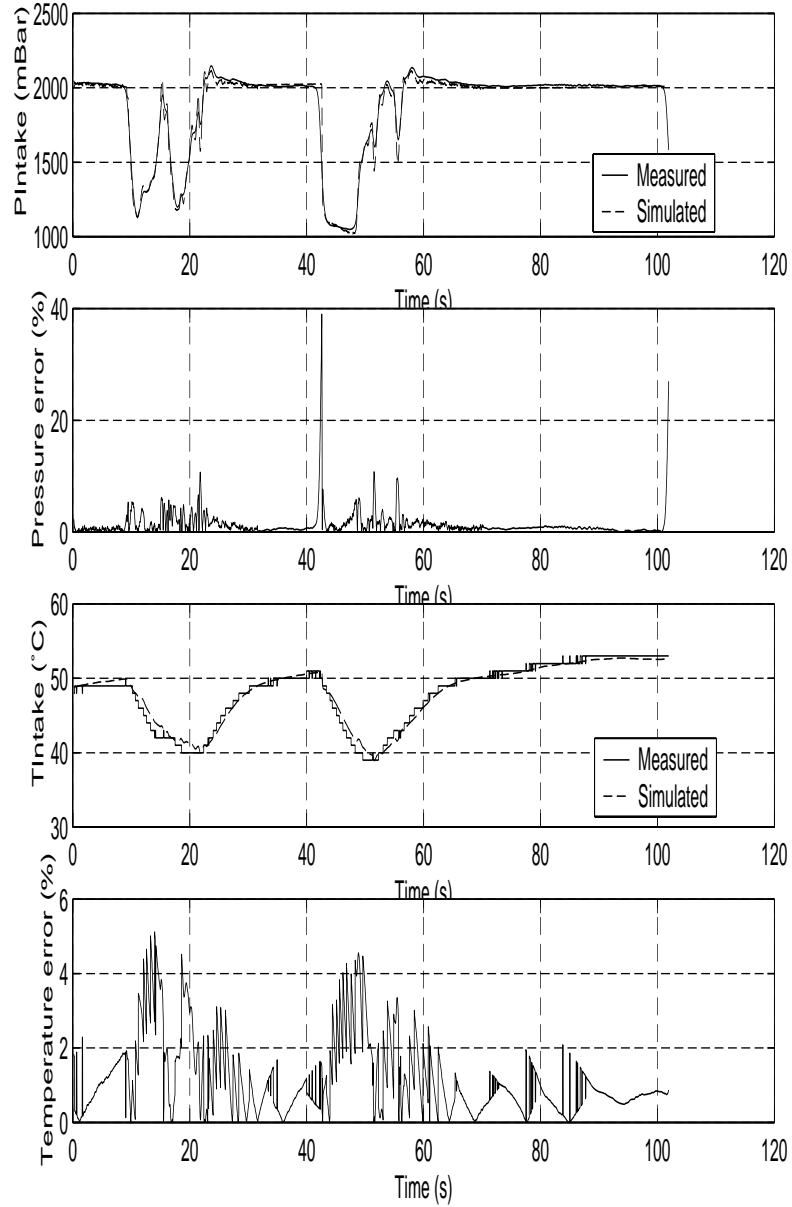
Figure A.24: Comparison between the p&T state model including heat transfer and measurements when EGR is not active. Simulation file 1.

Figure A.25: Comparison between the p&T state model including heat transfer and measurements when EGR is not active. Simulation file 3.

Figure A.26: Comparison between the p&T state model including heat transfer and measurements when EGR is not active. Simulation file 4.
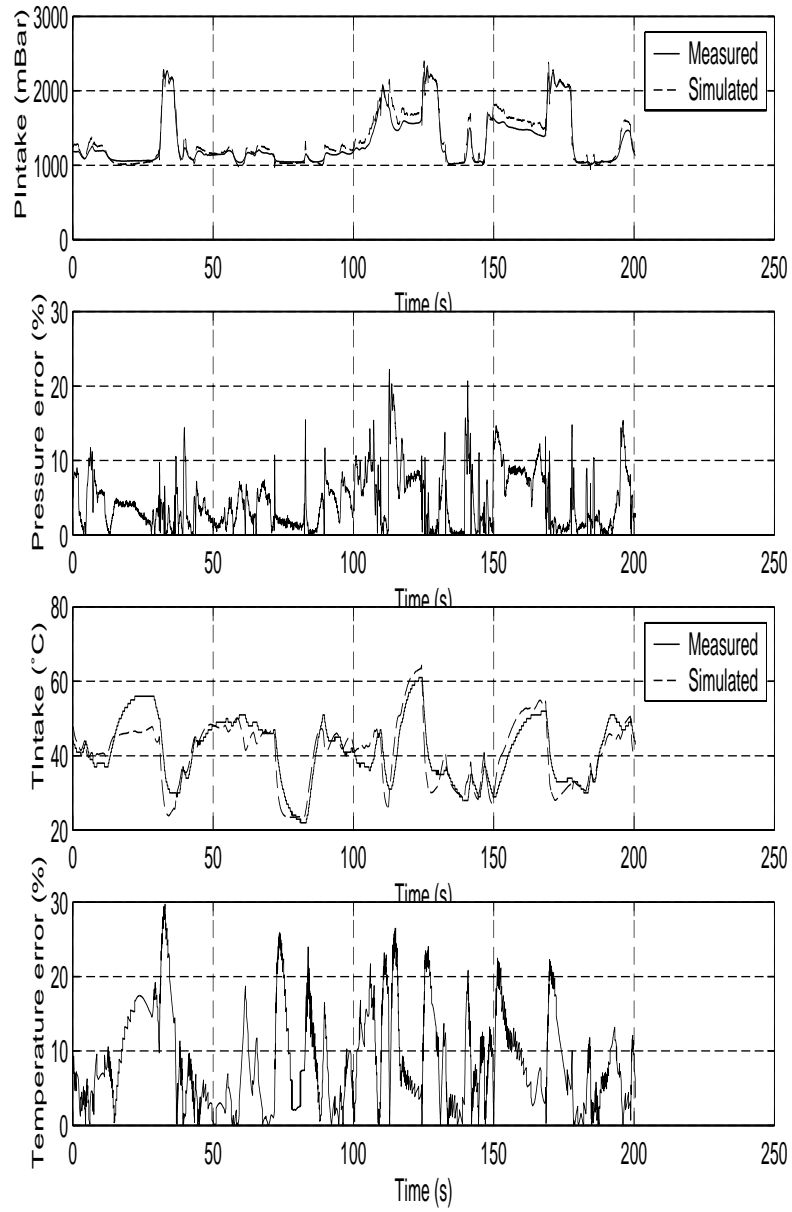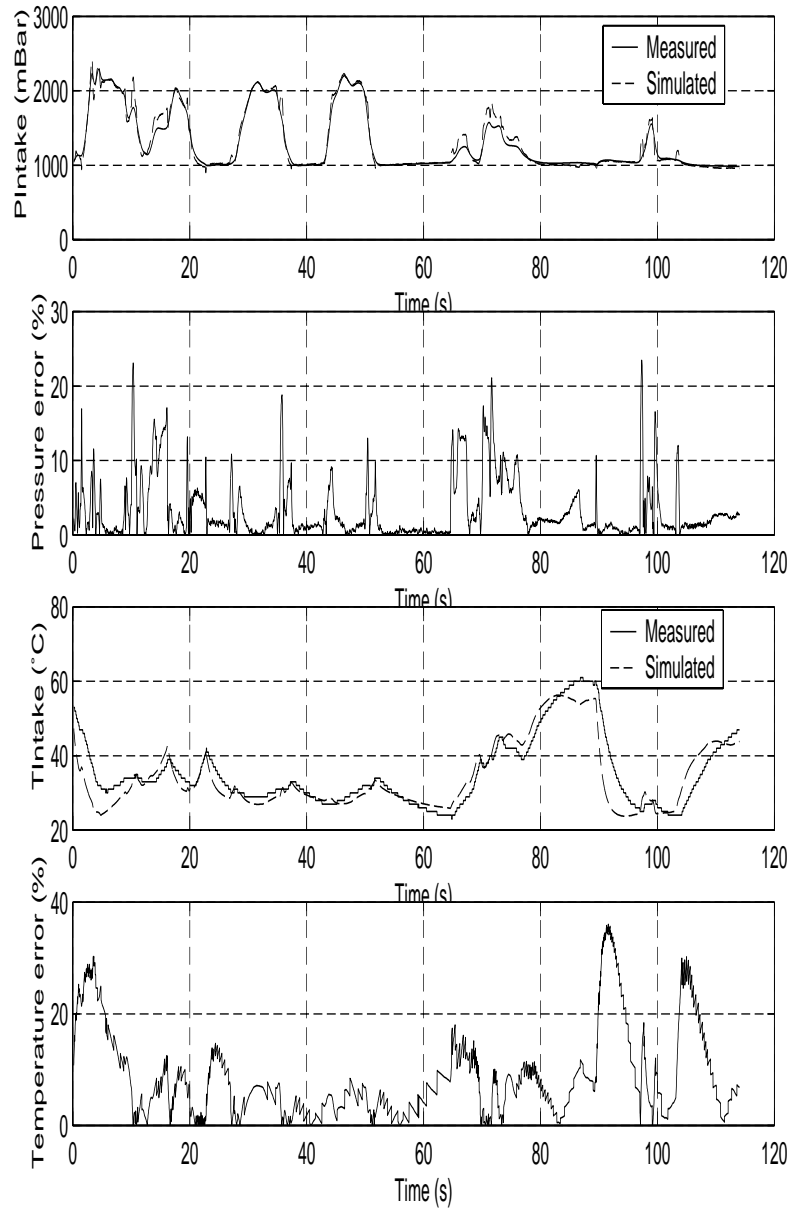
Figure A.27: Comparison between the p&T state model including heat transfer and measurements when EGR is not active. Simulation file 5.

Figure A.28: Comparison between the p&T state model including heat transfer and measurements when EGR is not active. Simulation file 6.

Figure A.29: Comparison between the p&T state model including heat transfer and measurements when EGR is active. Simulation file 8.

Figure A.30: Comparison between the p&T state model including heat transfer and measurements when EGR is active. Simulation file 9.

Appendix B: Simulink models

The equations derived for the intake manifold models in chapter 4 are implemented in simulink for easy simulation. How they are implemented are shown in this section.

The two models based on pressure and temperature are implemented in the same way. The only difference is the part simulating heat transfer. This part can be activated or deactivated by changing the value of the heat transfer coefficient (h_{HT}). When it is set to zero heat transfer is not included in the model.
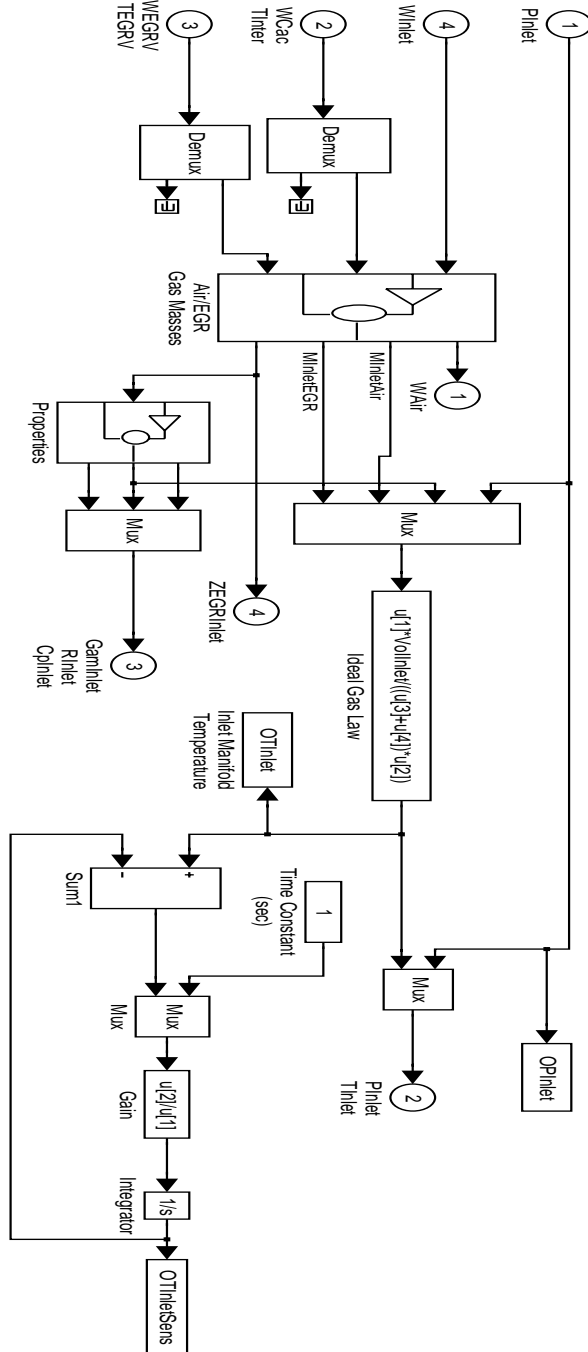
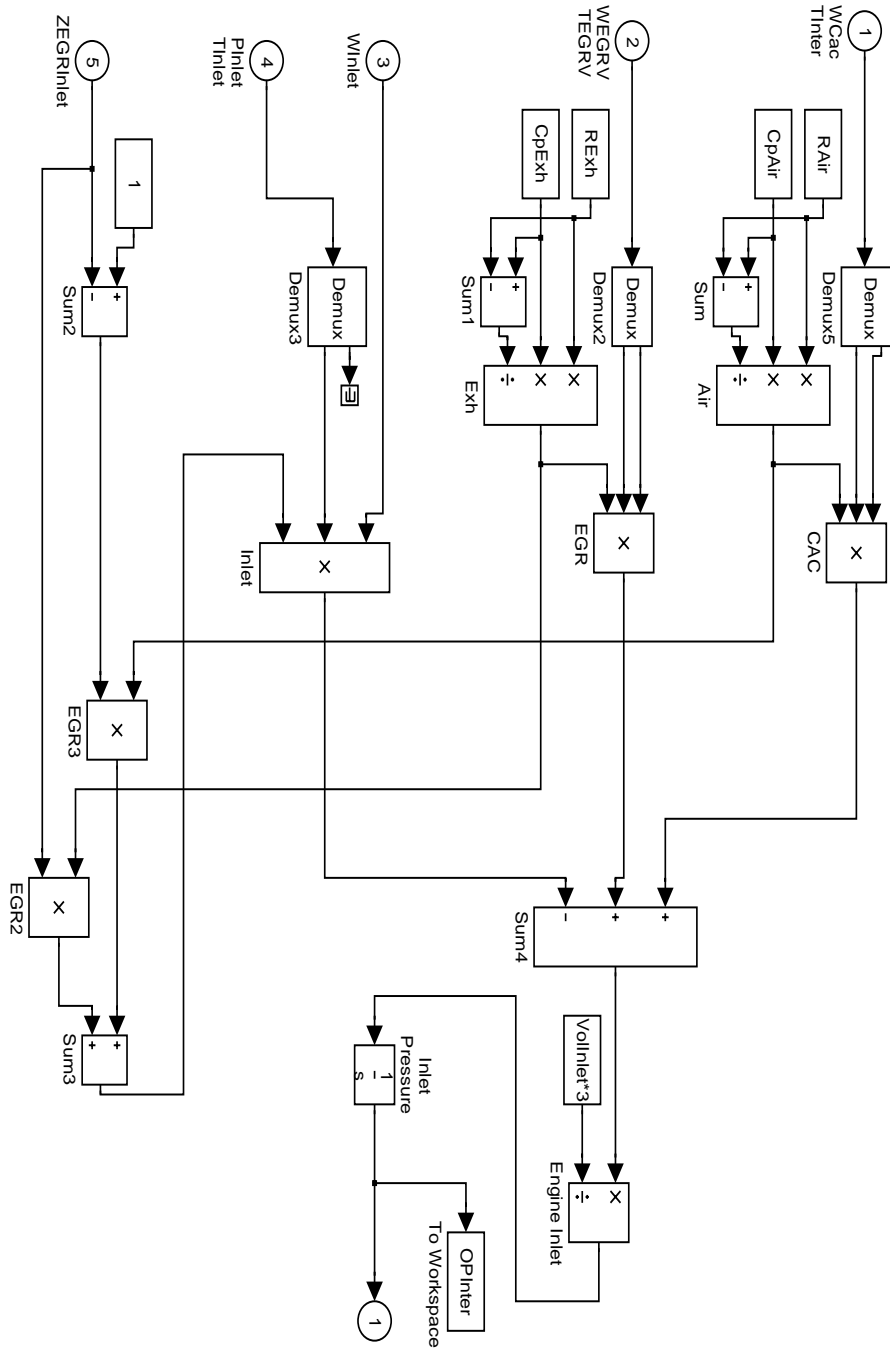Figure B.1: Implementation of the temperature calculation for the p&m state model. Equation 4.14.

Figure B.2: Simulink implementation of the pressure state equation for the p&m state model. Equation 4.11.
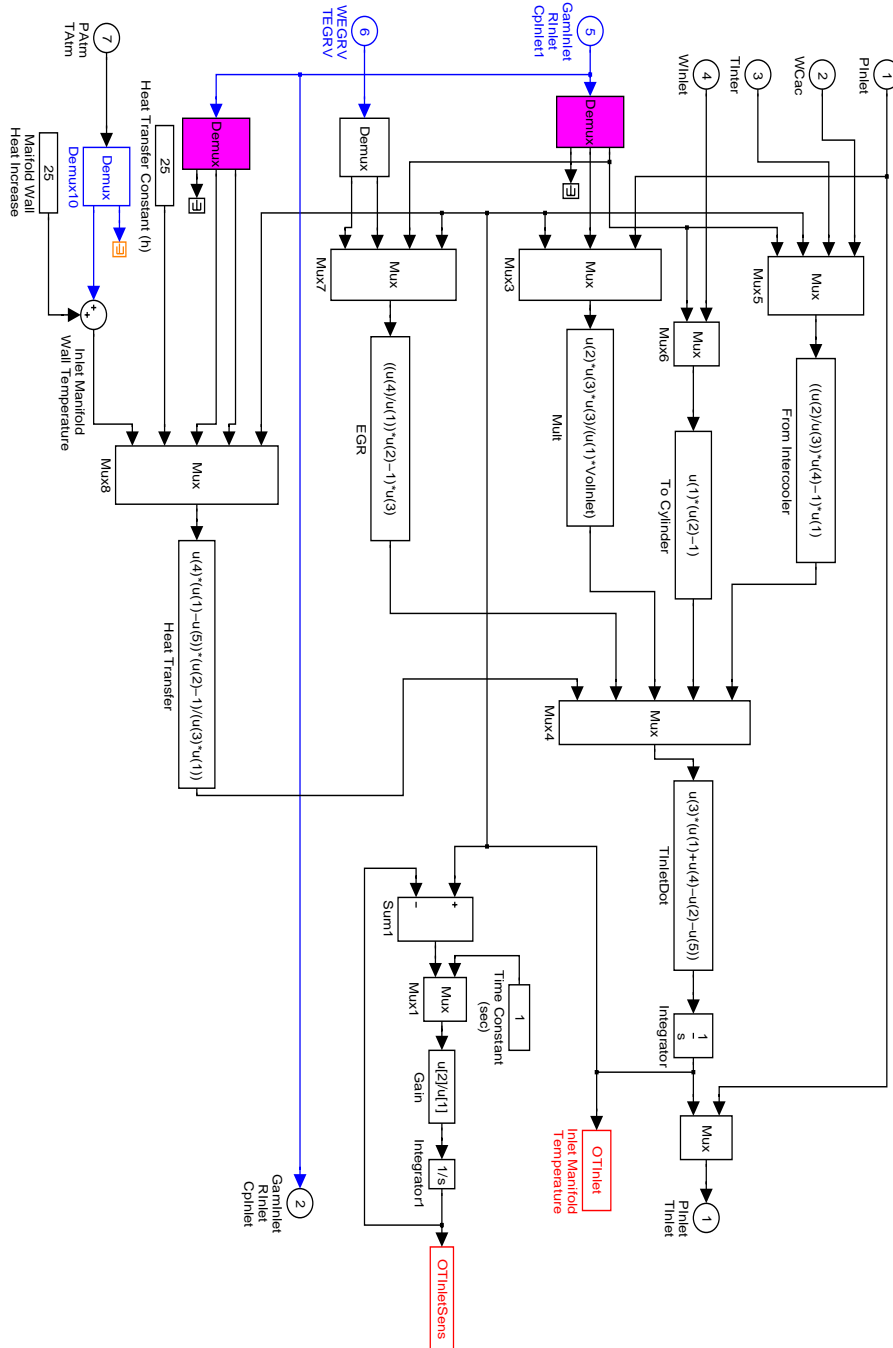
Figure B.3: Simulink implementation of the temperature state equation for the two models based on pressure and temperature. Equations 4.19 and 4.25.
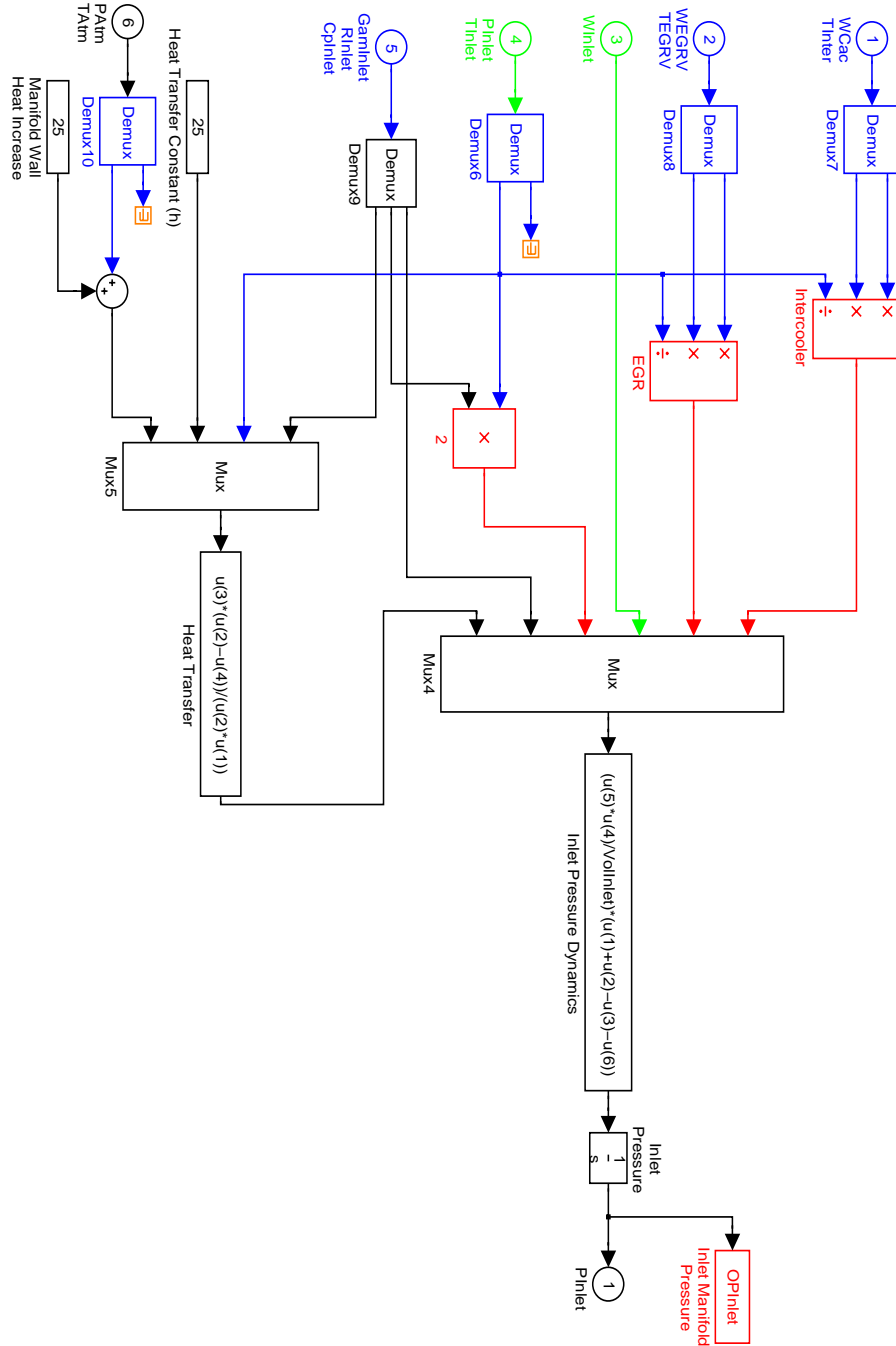
Figure B.4: Simulink implementation of the pressure state equation for the two models based on pressure and temperature. Equations 4.21 and 4.26.